

Heat-evoked activation of TRPA1

Kurganov, Erkin

Doctor of Philosophy

Department of Physiological Sciences,

School of Life Science,

SOKENDAI (The Graduate University for Advanced Studies)

Table of contents

1. Abstract	2
2. Introduction	4
3. Material and Methods	9
4. Results	13
Temperature and chemical sensitivity of green anole TRPA1	
Heat-evoked gaTRPA1 activation requires extracellular Ca ²⁺	
Synergistic effects of AITC and heat on green anole TRPA1	
Heat and AITC activate gaTRPA1 in excised inside-out patches	
AITC activates gaTRPA1 channels in excised inside-out patches in the absence of extracellular Ca ²⁺	
Extracellular Ca ²⁺ -dependent heat activation of gaTRPA1	
Extracellular Ca ²⁺ is not essential for heat activation of chicken and rat snake TRPA1	
A single mutation within the pore vestibule participates in gaTRPA1 heat activation	
Conserved residues near the extracellular face of TRPA1 transmembrane helix 2 are needed for heat-induced activation	
5. Discussion	24
6. References	31
7. Figure Legends	41
8. Tables and Figures	49
9. Acknowledgements	63

Abstract

Transient receptor potential ankyrin 1 (TRPA1) is a homotetrameric nonselective cation-permeable channel with six transmembrane domains and cytoplasmic N- and C-termini. The N-terminus is characterized by an unusually large number of ankyrin repeats. TRPA1 was initially identified as a potential mediator of noxious cold stimuli in mammalian nociceptive sensory neurons. Meanwhile, TRPA1s from non-mammalian vertebrates (snakes, green anole lizards, frogs and chickens) are activated by heat, but not cold stimulus. Although the 3-dimensional structure of human TRPA1 has been determined and TRPA1 channels from insects to birds are known to be activated by heat stimulus, the mechanism for temperature-dependent TRPA1 activation is unclear. The aim of this thesis work is to investigate whether TRPA1 is activated by heat directly and how extracellular Ca^{2+} is involved in heat-evoked activation of TRPA1. The detailed properties of green anole TRPA1 channel (gaTRPA1) expressed in HEK293T cells exposed to thermal and chemical stimulation were first examined in whole-cell and single-channel recordings. Arrhenius plots showed heat-evoked activation of gaTRPA1 with an activation temperature threshold of 35.8 °C, whereas heat together with the chemical agonist allyl isothiocyanate (AITC) had synergistic effects on gaTRPA1 channel activation in that either the temperature threshold or activating AITC concentration was reduced in the presence of the other stimulus. To investigate whether heat directly activates gaTRPA1 channels, excised inside-out membrane patches from gaTRPA1-expressing HEK293T cells were analyzed by the patch-clamp method. These measurements showed that heat and AITC directly activate gaTRPA1 channels. A comparison of the kinetics of heat- and AITC-evoked single-channel currents revealed that heat-activated currents had shorter open and closed times than those for AITC, thus indicating different activation mechanisms of heat and AITC. Significant heat-evoked gaTRPA1 activation was observed in the presence, but not absence, of extracellular Ca^{2+} . To understand the role of

extracellular Ca^{2+} in heat-evoked activation of TRPA1 channels, the extracellular Ca^{2+} -dependent heat sensitivity of gaTRPA1 was compared with the heat-activated TRPA1 channels from rat snake (rsTRPA1) and chicken (chTRPA1). In the absence of extracellular Ca^{2+} , rsTRPA1 and chTRPA1 were activated by heat and generated small inward currents at -60 mV. A comparison of extracellular amino acids in TRPA1 from these three species (gaTRPA1, chTRPA1 and rsTRPA1) identified three negatively charged amino acid residues (glutamate and aspartate) near the outer pore vestibule that are involved in heat-evoked TRPA1 activation in the presence of extracellular Ca^{2+} . These results suggest that neutralization of acidic amino acids by extracellular Ca^{2+} is important for heat-evoked activation of gaTRPA1, chTRPA1, and rsTRPA1, which could clarify mechanisms of heat-evoked channel activation.

Introduction

Transient receptor potential (TRP) channels are nonselective cation-permeable channels that can be categorized into 7 subfamilies: TRPC (canonical), TRPV (vanilloid), TRPA (ankyrin), TRPM (melastatin), TRPP (polycystin), TRPML (mucolipin) and TRPN (NOMPC) (not found in mammals) (Wu *et al.*, 2010). Over the last two decades, TRP ion channels were identified as molecular sensors for many different ambient stimuli, including temperature. The temperature sensitivity of TRP ion channel family members varies. For example, TRP vanilloid (TRPV) 1-4 (Caterina *et al.*, 1997; Caterina *et al.*, 1999; Guler *et al.*, 2002; Peier *et al.*, 2002b; Smith *et al.*, 2002; Xu *et al.*, 2002) and TRP melastatin (TRPM) 2-5 (Talavera *et al.*, 2005; Togashi *et al.*, 2006; Vriens *et al.*, 2011) are activated by hot and warm temperatures. Meanwhile, TRPM8 and TRP canonical (TRPC) 5 in mice and humans are activated by cold stimulus (McKemy *et al.*, 2002; Peier *et al.*, 2002a; Zimmermann *et al.*, 2011). TRPA1, a unique member of the ankyrin subfamily, was initially identified as a potential mediator of noxious cold stimulus in mouse nociceptive sensory neurons (Story *et al.*, 2003). This hypothesis was based on the observation that TRPA1 responds to cold stimulus in heterologous expression systems, although other recent studies did not observe TRPA1 cold sensitivity (Jordt *et al.*, 2004; Nagata *et al.*, 2005). Although many TRP channel family members contain between 3 and 6 ankyrin repeats (ARs) in the N-terminal region, TRPA1 is distinguished by having an unusually large (16-17) number of AR repeats (Cordero-Morales *et al.*, 2011). The *trpa1* gene was first cloned from lung fibroblasts (Jaquemar *et al.*, 1999) and was originally named ANKTM1 because of these multiple N-terminal ankyrin repeats (Story *et al.*, 2003). TRPA1 is primarily expressed in dorsal root ganglia (DRG) as well as trigeminal ganglia (TG) and nodose ganglia in mammals, where it was reported to respond to noxious cold and some pungent chemicals (Story *et al.*, 2003; Bautista *et al.*, 2005). TRPA1 is a homotetrameric nonselective cation permeable channel

with six transmembrane domains (Gaudet, 2008; Paulsen *et al.*, 2015) that functions as a polymodal receptor to detect various noxious (pungent) chemicals such as allyl isothiocyanate (AITC), piperin, allicin, cinnamaldehyde (CA), sanshool, oleocanthal, carvacrol and miogadial contained in mustard oil, black pepper, garlic, cinnamon, Japanese pepper (Sansho), olive oil, oregano and Zingiber mioga (Bandell *et al.*, 2004; Jordt *et al.*, 2004; Macpherson *et al.*, 2005; Koo *et al.*, 2007; Iwasaki *et al.*, 2009; Okumura *et al.*, 2010; Peyrot des Gachons *et al.*, 2011). TRPA1 activity is inhibited by 1,8-cineole and borneol contained in some plants (Takaishi *et al.*, 2012; Takaishi *et al.*, 2014). The channels also respond to mechanical stimulus (Kwan *et al.*, 2006), intracellular alkalization (Fujita *et al.*, 2008), and hyperosmotic stress (Zhang *et al.*, 2008).

TRPA1 has been linked to several painful sensations and diseases, such as inflammatory pain, cold hyperalgesia, mechanical pain, mechanical hypersensitivity, inflammatory pain, and asthmatic airway inflammation (Bandell *et al.*, 2004; Jordt *et al.*, 2004; Nagata *et al.*, 2005; Bautista *et al.*, 2006; Kwan *et al.*, 2006; Caceres *et al.*, 2009), and *trpa1*^{-/-} mice or mice treated with TRPA1 antagonists showed reduced pain behaviors or inflammation. TRPA1 is also involved in Familial Episodic Pain Syndrome (FEPS), an inherited disease that occurs in people from Columbia who carries a point mutation in TRPA1 (N855S) (Kremeyer *et al.*, 2010). The biophysical properties of TRPA1 N855S differ from wild type by showing increased inward currents upon stimulation with TRPA1 agonists or at normal resting potentials.

As TRPA1 is involved in various types of pain and diseases, drugs that can inhibit TRPA1 channel activity are necessary in the medical sphere. Unlike TRPA1 activators, few TRPA1 inhibitors have been studied. Whereas AP-18 [(Z)-4-(4-chlorophenyl)-3-methylbut-3-en-2-oxime] inhibits TRPA1 and reduces inflammatory pain in vivo (Petrus *et al.*, 2007), A-967079 [(R)-8-[4-methyl-5-(4-trifluoromethylphenyl)-oxazol-2-ylamino]-1,2,3,4-

tetrahydronaphthalen-2-ol)], which is similar to AP-18 except for a replacement of the chloro-phenyl of AP-18 with fluor-phenyl at the para position and for its binding to F909 in hTRPA1 (Paulsen *et al.*, 2015), prevented calcium influx through TRPA1 channels at low concentrations (Chen *et al.*, 2011). Another TRPA1 inhibitor, HC-030031 [2-(1,3-dimethyl-2,6-dioxo-1,2,3,6-tetrahydro-7H-purin-7-yl)-N-(4-isopropylphenyl)acetamide], and its analog Chembridge-5861528, also inhibit TRPA1 at micromolar concentrations (McNamara *et al.*, 2007; Eid *et al.*, 2008; Wei *et al.*, 2009; Gupta *et al.*, 2016).

The physiological role of TRPA1 as a thermoreceptor in sensory transduction is currently the subject of spirited debate. The response of TRPA1 to temperature shows species-specific differences. Several studies showed that mouse TRPA1 is a thermosensitive TRP channel that is activated by noxious cold both *in vitro* (Story *et al.*, 2003) and *in vivo* (Karashima *et al.*, 2009), while other studies found no cold activation of TRPA1 (Jordt *et al.*, 2004; Zurborg *et al.*, 2007). A comparison of mouse and *Drosophila* TRPA1s showed opposing TRPA1 thermosensitivity (Viswanath *et al.*, 2003), suggesting that these two TRPA1s are not functional orthologues. Moreover, TRPA1 expressed by different snake species (Gracheva *et al.*, 2010), fly (Kang *et al.*, 2012), frog, lizard, and chicken (Saito *et al.*, 2012; Kurganov *et al.*, 2014; Saito *et al.*, 2014) are activated by heat, but not cold. However, whether vertebrate heat-activated TRPA1 is directly activated by temperature remains unclear. Therefore, one of my focuses was to study direct/indirect activation of TRPA1 by heat stimulus.

On the other hand, it was suggested that all thermosensitive TRP channels have a U-shaped activation profile, which would explain the finding that all heat-activated TRP channels also show activation in response to cold (Clapham & Miller, 2011). Several groups provided experimental evidence for a U-shaped thermosensitive response of TRPA1 (Moparthy *et al.*, 2014; Moparthy *et al.*, 2016), while other studies reported that hTRPA1 is not a thermosensitive channel (Chen *et al.*, 2013). Meanwhile, some groups proposed allosteric

gating and coupling models to explain temperature-evoked activation of TRPA1 channels (Salazar *et al.*, 2011; Voets, 2012; Jara-Oseguera & Islas, 2013; Qin, 2013). As such, the mechanisms that mediate heat- or cold-activation of TRPA1 channel activity require additional clarification.

The chemical and temperature sensitivity of TRPA1 varies among species. Whereas the chemical sensitivity of TRPA1 from different species is similar, the temperature sensitivity remains puzzled. TRPA1 channel temperature sensitivity was studied in various species; such as insects (*Drosophila*, honeybee, mosquito and silkworm) (Viswanath *et al.*, 2003; Hamada *et al.*, 2008; Wang *et al.*, 2009; Kohno *et al.*, 2010; Kang *et al.*, 2011; Liu & Zwiebel, 2013; Sato *et al.*, 2014), vertebrates (frogs, lizards, snakes) (Gracheva *et al.*, 2010; Saito *et al.*, 2012; Kurganov *et al.*, 2014), birds (chicken) (Saito *et al.*, 2014), and mammals (mouse and human) (Story *et al.*, 2003; Moparthi *et al.*, 2014). Recently, the evolutionary aspects (from insects to mammals) of temperature-dependent TRPA1 channel activity were reported and rationales for the loss or changes in TRPA1 temperature sensitivity were proposed (Laursen *et al.*, 2015; Saito & Tominaga, 2015).

Ca^{2+} acts as a permeant ion and an intracellular modulator of various TRP channels. The importance of intracellular and extracellular Ca^{2+} for both activation and modulation of TRPA1 has been reported (Jordt *et al.*, 2004; Doerner *et al.*, 2007; Zurborg *et al.*, 2007; Wang *et al.*, 2008; Karashima *et al.*, 2009). However, whether extracellular Ca^{2+} plays a role in temperature-dependent gating of TRPA1 channels is unclear.

In this thesis work I characterized the thermal and chemical sensitivity of gaTRPA1 channels expressed in HEK293T cells. I found that gaTRPA1 was activated by heat and chemical stimuli, and that these two stimuli act synergistically. In addition, the gaTRPA1 channel was activated by heat and AITC in excised membrane patches, indicating that gaTRPA1 is activated by these stimuli in a membrane-delimited manner. Furthermore, I

investigated the role of extracellular cations in the heat-evoked activation of TRPA1 and identified several negatively charged amino acids near the opening of the ion channel pore that are necessary for heat-evoked activation of gaTRPA1, chicken TRPA1 and rat snake TRPA1. Based on my data, I propose a new model for heat-evoked activation of TRPA1 with the involvement of extracellular Ca^{2+} .

Material and Methods

DNA

The entire coding regions of TRPA1 from green anole and chicken were previously cloned into pcDNA3.1 (Invitrogen; (Saito *et al.*, 2012; Saito *et al.*, 2014). Rat snake TRPA1 cDNA (Gracheva *et al.*, 2010) was a kind gift from David Julius (University of California San Francisco) and was subcloned into the pcDNA3.1 vector for HEK293 cell expression.

Cell culture

Human embryonic kidney-derived 293T (HEK 293T) cells were maintained at 37 °C and 5% CO₂ in Dulbecco's modified Eagle Medium (WAKO Pure Chemical Industries, Ltd.) containing 10% fetal bovine serum (Biowest SAS), 100 units/mL penicillin (Invitrogen Corp.), 100 µg/mL streptomycin (Invitrogen Corp.), and 2 mM GlutaMAX (Invitrogen Corp.). For patch-clamp recordings, 1 µg green anole, chicken, or rat snake TRPA1 plasmid DNA in pcDNA3.1 and 0.1 µg pGreen Lantern 1 cDNA were transfected to HEK293 cells cultured in 35 mm dishes using Lipofectamine Plus Reagent (Invitrogen Corp.). After incubating for 3–4 h, the cells were reseeded on cover slips and further incubated at 33 °C in 5% CO₂. Patch-clamp recordings were performed 1 day after transfection.

Chemicals

AITC was purchased from Kanto Chemical, Tokyo Chemical Industry and HC-030031 was purchased from Sigma. AITC was dissolved in methanol for stock solutions (1 M and 100 mM), and HC-030031 was dissolved in DMSO as a stock solution (10 mM) and diluted to the final concentration using bath solution.

Construction of mutant TRPA1 channels

TRPA1 point mutants were constructed according to the procedures described in the QuikChange site-directed mutagenesis kit (Stratagene) with minor modifications. Point mutations were introduced by PCR using the green anole-TRPA1/pcDNA3.1, chicken-TRPA1/pcDNA3.1, and rat snake-TRPA1/pcDNA3.1 vectors as templates with oligonucleotide primers containing the intended mutations (Table 1). The resulting amplified PCR products were cloned into pcDNA3.1, which was transformed into *Escherichia coli*, and pcDNA3.1 vectors containing TRPA1 with the desired mutations were then purified using standard procedures. The entire TRPA1 coding sequences were determined to confirm that only the intended mutations were introduced.

Electrophysiology

For whole-cell experiments the experimental solutions were: bath solution, 140 mM NaCl, 5 mM KCl, 2 mM MgCl₂, 2mM CaCl₂, 10 mM HEPES and 10 mM glucose, pH 7.4 adjusted with NaOH (for Ca²⁺-free experiments 5 mM EGTA was added instead of 2 mM CaCl₂); pipette solution, 140 mM KCl, 5 mM EGTA and 10 mM HEPES, pH 7.4 adjusted with KOH. In some experiments, the free calcium concentration of the pipette solution was maintained at 100 nM and 1 μM as calculated with the MAXC program (Stanford University). Data from whole-cell voltage-clamp recordings were acquired at 10 kHz and filtered at 5 kHz for analysis (Axon 200B amplifier with pCLAMP software, Axon Instruments, Foster City, CA, USA). The membrane potential was clamped at -60 mV and voltage ramp-pulses from -100 to +100 mV (500 ms) were applied every 5 s. Rectification ratios (positive voltages/negative voltages) were calculated by dividing current densities at +100 mV (positive potential) to -100 mV voltages. For inside-out experiments the solutions used were: bath solution, 140 mM NaCl, 5 mM KCl, 2 mM MgCl₂, 2 mM CaCl₂, 10 mM HEPES and 10 mM glucose, pH 7.4

adjusted with NaOH. Single-channel data were sampled at 10 kHz and filtered at 2 kHz, and analyzed using Clampfit 10.2 software. Single channel unitary current was determined from the best fit Gaussian distribution of amplitude histograms.

All experiments were performed at 25 °C unless otherwise stated. Heat stimulation was induced by increasing the bath temperature using a pre-heated solution warmed in an inline heater or heating stage (1 °C/s, with a maximum of 62 °C). The temperature was monitored using a thermocouple (TC-344; Warner Instruments, Hamden, CT, USA) placed within 100 μm of the patch-clamped cell. Temperature profiles and Arrhenius plots for the data from whole-cell voltage-clamp recordings were calculated using Origin software (Microcal). Temperature-sensitivity has been explained by a mechanism based on a fine balance of large changes in enthalpy and entropy (Voets *et al.*, 2004). Alternatively, temperature gating could be driven by changes in heat capacity (Clapham & Miller, 2011). Temperature-directionality could also be determined by the degree of allosteric coupling of a unidirectional temperature-sensor to the channel gate (Jara-Oseguera & Islas, 2013). Although the above mechanisms of temperature-activation differ substantially, we believe that thermal sensitivity (Q_{10}) is still a reliable marker to some extent. The absolute current values were plotted on a log scale against the reciprocal of the absolute temperature (T) (Arrhenius plot), and the temperature threshold for channel activation was determined by the temperature that caused a change in the slope.

Statistical analysis

Data in all figures are shown as means ± standard error of the mean (S.E.M.) or standard deviation (S.D.). Statistical analysis was performed by Student's t-test or analysis of variance (ANOVA) followed by a two-tailed multiple t-test with Bonferroni correction using Origin 8.5 software. Probability values (p) of < 0.05 were considered statistically significant.

3D structure modelling of gaTRPA1

Homology modelling of gaTRPA1 in the open state was performed using SWISS-MODEL (Automated Protein Modelling Server; (Arnold *et al.*, 2006; Bordoli *et al.*, 2009; Kiefer *et al.*, 2009)) and was based on a sequence alignment of amino acid residues 445-1078 of human TRPA1, for which the single-particle cryo-EM structure is known (Protein Data Bank accession number (3J5P); (Paulsen *et al.*, 2015)). The homology modelling data were used with PyMol (Schrödinger) to generate graphic presentations (Figs. 9B and 11).

Results

Temperature and chemical sensitivity of green anole TRPA1

The channel activity of gaTRPA1 expressed in HEK293T cells was examined using a whole-cell patch-clamp method. The thermal responsiveness of gaTRPA1 was tested by increasing the temperature of the perfusate from ~25 °C to ~45°C, which elicited a robust and rapidly activating inward current (at a negative holding potential) that was desensitized even by continuous heat stimulation, with the second heat stimulation evoking a smaller response (Fig. 1A). Stimulation with AITC, a chemical known to activate mammalian TRPA1 through covalent modification of cytosolic cysteine residues (Hinman *et al.*, 2006; Macpherson *et al.*, 2007), also elicited clear inward currents that were similar to the heat response with desensitization upon repetitive stimulation (Fig. 1B). When voltage-ramp pulses (500 ms) from -100 mV to +100 mV were applied every 5 s, the whole-cell recordings showed both heat- and AITC-evoked gaTRPA1-mediated inward currents at -60 mV with an outwardly rectifying current-voltage (I-V) relationship (Fig. 1C), indicating that heat- and AITC-evoked gaTRPA1 currents share this electrophysiological property. When the rectification ratios (positive voltages/negative voltages) were measured for heat- and AITC-evoked gaTRPA1 whole-cell currents, they both showed outward rectification (8.36 ± 1.26 , $n=6$ and 2.18 ± 0.21 , $n=7$ for heat- and AITC-evoked currents, respectively). To determine whether gaTRPA1 is a cold sensor, the thermal responsiveness of gaTRPA1 was tested by lowering the perfusate temperature from ~30 °C to ~12 °C with 100 nM free Ca²⁺ in the pipette solution, which together are purported to enhance TRPA1 activity. Whereas the cells responded to both heat and AITC stimulation, no cold-evoked currents in gaTRPA1-expressing HEK293T cells were observed (Fig. 1D).

Heat-evoked gaTRPA1 activation requires extracellular Ca²⁺

Since several TRP channels were reported to be activated or modulated by Ca²⁺ in various ways (McHugh *et al.*, 2003; Nilius *et al.*, 2006; Doerner *et al.*, 2007; Xiao *et al.*, 2008), the effect of extracellular Ca²⁺ on the heat- and AITC-evoked activation of gaTRPA1 was examined. Whole-cell patch-clamp recordings in HEK293T cells expressing gaTRPA1 were performed in the absence of extracellular Ca²⁺ and presence of heat stimulation applied by increasing the perfusate temperature from ~25 °C to ~45 °C, which evoked very small currents. Meanwhile, large inward currents were elicited by AITC stimulation in the same cell at -60 mV (Fig. 2A), suggesting that extracellular Ca²⁺ is required to produce significant gaTRPA1 currents during the heating. Heat-evoked currents in the presence of extracellular Ca²⁺ were significantly larger than those without extracellular Ca²⁺ (Fig. 2B; 199 ± 39 pA/pF, n = 6 and 12 ± 6 pA/pF, n = 6 in the presence and absence of extracellular Ca²⁺, respectively, p < 0.01). Although intracellular Ca²⁺ was previously shown to affect TRPA1 channel function (Doerner *et al.*, 2007; Zurborg *et al.*, 2007), here an increase in intracellular Ca²⁺ to 100 nM did not affect heat-evoked activation of gaTRPA1 expressed in HEK293 cells (15 ± 2.2 pA/pF, n = 5). Voltage-ramp pulses (500 ms) from -100 mV to +100 mV every 5 s were then applied, which again produced very small heat-evoked currents and large AITC-evoked gaTRPA1-mediated inward currents at negative potentials with an outwardly rectifying I-V relationship (Fig. 2A, C). Because gaTRPA1 was activated by AITC even in the absence of extracellular Ca²⁺, whether AITC-evoked currents differ in the presence and absence of extracellular Ca²⁺ was examined. Although stimulation with AITC elicited large inward currents at -60 mV that were similar to those shown in Fig. 1B, the inactivation became slow with half-inactivation (t_{half}) (1.05 ± 0.22 sec, n = 8 and 20.9 ± 3.32 sec, n = 8 in the presence and absence of extracellular Ca²⁺, respectively, p < 0.01) (Fig. 2D, F) in the absence of extracellular Ca²⁺. However, there was no difference in the current sizes of initial AITC-

evoked channels (420 ± 71 pA/pF, $n = 6$ and 423 ± 73 pA/pF, $n = 6$ in the presence and absence of extracellular Ca^{2+} , respectively) (Fig. 2E) or ratios of the 2nd to 1st currents (0.26 ± 0.03 pA/pF, $n = 6$ and 0.24 ± 0.02 pA/pF, $n = 6$ in the presence and absence of extracellular Ca^{2+} , respectively) (Fig. 2G) in both the presence and absence of extracellular Ca^{2+} , suggesting that extracellular Ca^{2+} does not affect the desensitization with repeated stimulation. These results indicated that extracellular Ca^{2+} plays a minor role in AITC-induced gaTRPA1 activation.

Synergistic effects of AITC and heat on green anole TRPA1

Because increased temperature was expected to affect AITC sensitivity, the dose-dependent profiles of gaTRPA1 activation by AITC at 25 °C and 30 °C was next examined,. The half-maximal effective concentration of AITC (EC_{50}) for gaTRPA1 activation at 25 °C was 394 ± 51 μM ($n = 6$), whereas elevation of the temperature to 30 °C increased the potency of AITC and produced an EC_{50} of 270 ± 40 μM ($n = 6$) without changes in efficacy (Fig. 3A). The current densities differed significantly between AITC concentrations of 300 and 600 μM (Fig. 3A). Dose-response curves compiled for individual cells showed that the AITC EC_{50} values at 25 °C and 30 °C were 468 ± 41 μM ($n = 5$) and 272 ± 36 μM ($n = 5$), respectively, which are similar to the above values and again significantly different from each other.

Arrhenius plots were then constructed to determine the temperature threshold for gaTRPA1 activation by heat without or with a low concentration of AITC (20 μM) that does not induce gaTRPA1 activation (Fig. 3A). Whereas the average temperature threshold for activation by heat stimulation was 35.8 ± 0.5 °C without AITC ($n = 6$, Fig. 3B and E), the threshold was significantly lower in the presence of AITC (26.9 ± 0.4 °C, $n = 6$, Fig. 3C and E, $p < 0.01$), which is a synergistic effect that is similar to that observed for AITC dependence at different temperatures (Fig. 3A). In addition, there was no significant

difference in temperature thresholds at two different basal temperatures (15-18 °C and 25 °C, n = 6, Fig. 3B, D and E), suggesting that the absolute temperature rather than the amount of temperature increase is important for gaTRPA1 activation, which is consistent with that seen for other thermosensitive TRP channels (Kashio *et al.*, 2012; Komatsu *et al.*, 2012). This AITC-induced reduction in temperature thresholds for gaTRPA1 activation can be viewed as a “sensitization”.

Heat and AITC activate gaTRPA1 in excised inside-out patches

In whole-cell recordings, many receptors or ion channel proteins might be modulated by intracellular processes or factors. To reduce the possibility that cytosolic factors might influence channel behaviors, heat- and AITC-mediated activation of gaTRPA1 channels in patches excised from transfected HEK293T cells in an inside-out configuration was next assessed. When the temperature was elevated from 25 °C, the basal level was shifted and clear single-channel openings could be observed in the excised patches. However, the single-channel activity was decreased even in the presence of heat stimulation (Fig. 4A), which could be viewed as a run-down. On the other hand, AITC-evoked single-channel openings with longer durations persisted even after AITC wash out, which could be due to the lipophilic nature of AITC (Fig. 4B). The Fig. 4A and B insets demonstrate before (*inset 1*), during (*inset 2*) and after (*inset 3*) applications of heat and AITC, and show clearer single-channel openings in the expanded traces. Although these results suggest that gaTRPA1 can be activated directly by heat or AITC, their opening kinetics has different characteristics (Fig. 4C and D). Heat- and AITC-activated channels, especially those that are heat-evoked, showed a small proportion of low-conductance channels at high voltages (e.g. ± 100 mV), which could correspond to the sub-conducting channels that have been reported for the heat-activated channels dTRPA1 (Wang *et al.*, 2013) and rTRPV1 (Nagy & Rang, 1999). Unitary

amplitudes of the heat-activated currents at a membrane potential of +100 mV and -100 mV were 10.2 pA and 4.87 pA, resulting in single-channel conductance of 102 ± 2.9 pS and 48.7 ± 1.3 pS, respectively ($n = 6$, Fig. 4C and E). Unitary amplitudes of the AITC-activated currents at +100 mV and -100 mV were 9.8 pA and 4.29 pA, resulting in single-channel conductance of 98.4 ± 0.9 pS and 42.9 ± 0.7 pS, respectively ($n = 6$, Fig. 4D and F), which are similar to the values observed for the heat-evoked responses. Accordingly, the I-V relationship for both heat- and AITC-activated single-channel openings showed similar outward rectifications that resembled those observed in whole-cell recordings. The outward rectification at the single-channel level might partially explain the outward rectification seen at the whole-cell level. Because the single-channel openings differed (Fig. 4), a more detailed analysis of single-channel currents was performed. Surprisingly, a distinct difference in the open-time distributions of heat- and AITC-activated currents was observed (Fig. 5A and B). The average open-times (τ_{open}) of the heat-activated currents ($\tau = 0.44 \pm 0.14$ msec) were significantly shorter than those of AITC-activated currents ($\tau = 2.87 \pm 0.83$ msec) (Fig. 5C-E). The closed-time distributions similarly differed between the heat-activated currents ($\tau_1 = 4.39 \pm 1.05$ msec) and the AITC-activated currents ($\tau_1 = 25.2 \pm 4.95$ msec) (Fig. 5F - H). These results clearly indicated that heat-activated channels open and close with shorter durations compared with AITC-activated channels.

AITC activates gaTRPA1 channels in excised inside-out patches in the absence of extracellular Ca²⁺

Because gaTRPA1 activation by AITC stimulation in the presence and absence of extracellular Ca²⁺ was quite similar at a whole-cell level, the properties of AITC-evoked gaTRPA1 channel activation were examined at a single-channel level. In the inside-out patch configuration, AITC evoked single-channel currents in the absence of extracellular Ca²⁺ that

were similar to those observed in the presence of extracellular Ca^{2+} (Fig. 6A). Meanwhile, almost no heat-evoked single-channel current activation was observed in the absence of extracellular Ca^{2+} in the pipette (data not shown). The Fig. 6A insets demonstrate before (*inset 1*), during (*inset 2*) and after (*inset 3*) AITC application. The amplitudes (4.2 ± 0.1 pA, $n = 6$ and 4.13 ± 0.27 pA, $n = 5$ in the presence and absence of extracellular Ca^{2+} , respectively) (Fig. 6B and C), open-time distributions ($\tau = 2.87 \pm 0.83$ msec, $n=5$ and 2.23 ± 0.6 msec, $n = 5$ for the τ of the open-time, in the presence and absence of extracellular Ca^{2+} , respectively) (Fig. 6D and E) and closed-time distributions ($\tau_1 = 25.2 \pm 4.95$ msec, $n=4$ and 17.86 ± 2.04 msec, $n = 5$ for the τ of the closed-time, in the presence and absence of extracellular Ca^{2+} , respectively) (Fig. 6F and G) were quite similar in the presence and absence of extracellular Ca^{2+} . These results suggested that extracellular Ca^{2+} does not affect the properties of gaTRPA1-mediated single-channel currents that are activated by AITC.

Extracellular Ca^{2+} -dependent heat activation of gaTRPA1

Whole-cell and inside-out single-channel recordings in HEK293T cells expressing gaTRPA1 showed both heat and AITC-evoked current activation. Temperature-evoked gaTRPA1 currents were not observed in the absence of extracellular Ca^{2+} , although these cells did respond to AITC stimulation. To explore how extracellular Ca^{2+} is involved in heat-evoked activation of gaTRPA1, gaTRPA1 channel activation was first examined upon heat stimulation using a high concentration (1 μM) of intracellular free Ca^{2+} in the pipette solution because intracellular Ca^{2+} is known to affect TRPA1 channel function (Jordt *et al.*, 2004; Doerner *et al.*, 2007; Zurborg *et al.*, 2007). In the whole-cell configuration, negligible inward currents were observed at -60 mV following heat stimulation (from 25 °C to over 45 °C) with 1 μM intracellular Ca^{2+} (Fig. 7A) or without intracellular Ca^{2+} (Fig. 7B) in the absence of extracellular Ca^{2+} , yet gaTRPA1 channels responded to AITC (400 μM) with large inward

currents. This activation is known to occur through covalent modification of cytosolic cysteine residues of TRPA1 (Macpherson *et al.*, 2005; Hinman *et al.*, 2006) and was inhibited by the TRPA1-specific antagonist HC-030031 (50 μ M) (Fig. 7A). I next tested whether other divalent cations are involved in heat-evoked activation of gaTRPA1. The absence of extracellular Mg^{2+} did not affect the heat-evoked activation of gaTRPA1 (Fig. 7C). Substitution of extracellular Ca^{2+} with another divalent cation, Ba^{2+} , did not evoke gaTRPA1 currents upon heat stimulation, but AITC-evoked currents were induced (Fig. 7D), suggesting that heat-evoked activation of gaTRPA1 channel is solely dependent on extracellular Ca^{2+} . To gain more information on the dependency of TRPA1 heat activation on extracellular Ca^{2+} , channel activity was recorded in the presence of increasing extracellular Ca^{2+} concentrations (0 to 2 mM) under heat stimulation. The current densities of the heat-evoked gaTRPA1 currents were significantly increased with increasing extracellular Ca^{2+} concentrations (Fig. 7E and F). However, the temperature thresholds for heat-evoked gaTRPA1 activation did not differ between 1 and 2 mM extracellular Ca^{2+} (34.6 ± 1.5 °C, $n=5$ and 35.8 ± 0.5 °C, $n=6$, respectively) (Fig. 7G-I). These results suggested that extracellular, but not intracellular, Ca^{2+} ions are important for heat activation of gaTRPA1.

Extracellular Ca^{2+} is not essential for heat activation of chicken and rat snake TRPA1

To find the residue(s) responsible for heat-evoked gaTRPA1 activation in the presence of extracellular Ca^{2+} , heat-evoked currents of TRPA1 from different species were examined. Based on the finding that chicken TRPA1 (chTRPA1) and rat snake TRPA1 (rsTRPA1) expressed in *Xenopus oocytes* are activated by heat (Gracheva *et al.*, 2010; Saito *et al.*, 2014), the requirement of extracellular Ca^{2+} for heat-evoked activation of chTRPA1 and rsTRPA1 expressed in HEK293T cells was examined. The chTRPA1 and rsTRPA1 activation was first compared in the presence and absence of extracellular Ca^{2+} in whole-cell configurations at -

60 mV. Similar to gaTRPA1, large inward currents for both chTRPA1 (Fig. 8A) and rsTRPA1 (Fig. 8E) in the presence of extracellular Ca^{2+} were observed. Interestingly, small but significant inward currents were elicited upon heat stimulation even in the absence of extracellular Ca^{2+} for chTRPA1 (Fig. 8B) and rsTRPA1 channels (Fig. 8F), suggesting that heat-evoked TRPA1 activation in these species does not depend solely on extracellular Ca^{2+} . Although the heat-evoked currents were smaller in the absence of extracellular Ca^{2+} , temperature thresholds for heat-evoked activation of chTRPA1 and rsTRPA1 determined by constructing Arrhenius plots were unchanged in the presence and absence of extracellular Ca^{2+} (chTRPA1, 39.3 ± 0.5 °C, $n=5$ and 39.6 ± 1.2 °C, $n=6$, Fig. 8C and D; and rsTRPA1, 37.4 ± 0.9 °C, $n=6$ and 39 ± 0.6 °C, $n=6$, Fig. 8G and H).

A single mutation within the pore vestibule affects gaTRPA1 heat activation

Given the findings that gaTRPA1 heat activation requires extracellular, but not intracellular Ca^{2+} , and that heat-evoked activation of chTRPA1 and rsTRPA1 occurred even in the absence of extracellular Ca^{2+} , the TRPA1 amino acid sequences were compared for the three species (Fig. 9A). The finding that extracellular Ca^{2+} is required for channel activation following heat stimulation suggests that negatively charged amino acids located on the extracellular face of gaTRPA1, but not chTRPA1 or rsTRPA1, are involved in this heat-evoked activation. An amino acid alignment showed that gaTRPA1 has only one negatively charged glutamate at position 894 (in red in Fig. 9A), whereas the equivalent residues in chTRPA1 (897) and rsTRPA1 (895) are neutral glutamines (Fig. 9A). To understand the location of gaTRPA1 Glu894 in greater detail, homology modeling of gaTRPA1 was performed based on the cryo-EM structure of human TRPA1 (Paulsen *et al.*, 2015). The resulting model suggested that Glu894 is exposed to the extracellular side of the gaTRPA1 channel at the pore vestibule (Fig. 9B). As such, a gaTRPA1 channel with Glu894 mutated

to Gln (E894Q) was constructed and the channel activity of this mutant expressed in HEK293T cells following heat and chemical stimulations was analyzed. E894Q exhibited a large inward current upon heat application in the presence of extracellular Ca^{2+} , and a small but significant inward current was observed even in the absence of extracellular Ca^{2+} (Fig. 9C and D), suggesting that Glu894 of gaTRPA1 is involved in the heat-evoked activation of gaTRPA1 in the presence of extracellular Ca^{2+} . Although the sizes of the heat-evoked currents for E894Q differed in the presence and absence of extracellular Ca^{2+} , AITC-evoked currents were similar among wild type TRPA1 (420.2 ± 50.6 pA, $n=6$) in the presence of extracellular Ca^{2+} and TRPA1 E894Q in the presence (425.3 ± 67.9 pA, $n=5$) and absence (415.2 ± 81.5 pA, $n=6$) of extracellular Ca^{2+} (Fig. 9E). Moreover, changing Glu894 to positively charged Lys (E894K) conferred heat-evoked current activation in the absence (87.7 ± 15.3 pA, $n=6$) and presence (219.4 ± 26.5 pA, $n=5$) of extracellular Ca^{2+} (Fig. 9F and G), which was similar to that seen for E894Q, suggesting that neutralization of the negative charge is important for heat-evoked activation of gaTRPA1 in the absence of extracellular Ca^{2+} . To further confirm the importance of the negative charge at position 894 of gaTRPA1 for heat-evoked activation in the presence of extracellular Ca^{2+} , Gln897 in chicken TRPA1 and Gln895 in rat snakeTRPA1 were mutated to Glu. Interestingly, both Q897E (chTRPA1) and Q895E (rsTRPA1) mutants showed significantly smaller inward currents upon heat stimulation in the absence of extracellular Ca^{2+} (20.9 ± 6.3 pA, $n=4$ and 50.8 ± 11.9 pA, $n=5$, respectively) than did WT channels (Fig. 9I, J, L and M), whereas Q897E (chTRPA1) and Q895E (rsTRPA1) mutants showed large inward currents upon heat stimulation in the presence of extracellular Ca^{2+} (97.1 ± 16.5 pA, $n=5$ and 335.7 ± 22.2 pA, $n=5$, respectively) (Fig. 9H, J, K and M), which is similar to that seen for WT channels. These data suggested that more negative charges on the channel vestibule surface increase Ca^{2+} sensitivity of the channels to heat stimulation, as was seen for gaTRPA1. Together these results indicated that

AITC-induced activation of gaTRPA1 differs from temperature-induced activation and that a negatively charged amino acid is important for heat-evoked activation of TRPA1 channels in the presence of extracellular Ca^{2+} .

Conserved residues near the extracellular face of TRPA1 transmembrane helix 2 are needed for heat-induced channel activation

Since the gaTRPA1 E894Q mutant is similar to chTRPA1 and rsTRPA1 in that its heat-evoked currents are smaller in the absence of extracellular Ca^{2+} than in the presence of extracellular Ca^{2+} (Figs. 8 and 9), it was hypothesized that negatively charged amino acids at the extracellular side of the channel could be conserved across all three species (gaTRPA1, chTRPA1, and rsTRPA1). Further amino acid sequence alignment identified two candidate amino acids, Glu and Asp, before (green) and within (cyan) transmembrane pore helix 2 (Fig. 10A). To neutralize these charged amino acids, the Glu and Asp residues were mutated to Gln and Asn, respectively, and single, double, and triple mutants of the channels were made. As mentioned above (Fig. 9D), gaTRPA1 (E894Q) exhibited significantly larger heat-evoked currents at -60 mV in the absence of extracellular Ca^{2+} than wild type gaTRPA1 (97.8 ± 14.3 pA, $n=6$ vs. 11.9 ± 1.2 pA, $n=5$, $p < 0.05$) (Fig. 10C). Therefore, two double mutations (E894Q/D918N and E894Q/E922Q) and one triple mutation (E894Q/D918N/E922Q) were made in gaTRPA1. Although the two double mutations showed heat-evoked currents that were similar in size to the single mutation E894Q (E894Q/D918N, green, 125.6 ± 40.9 pA, $n=6$; E894Q/E922Q, cyan, 120.5 ± 38.7 pA, $n=5$) in the absence of extracellular Ca^{2+} , the triple mutant showed large inward currents upon heat stimulation in the absence (197.2 ± 41.1 pA, $n=5$, navy) and presence (200.4 ± 45.2 pA, $n=6$, pink) of extracellular Ca^{2+} , and the currents were similar in size to those of wild type gaTRPA1 currents in the presence of extracellular Ca^{2+} (199.1 ± 39.1 pA, $n=5$, black) (Fig. 10B and C). Unlike gaTRPA1, in the

absence of extracellular Ca^{2+} , chTRPA1 and rsTRPA1 channels were activated by heat with small inward currents (Fig. 9B and F). Thus, two single point mutants in chTRPA1 and rsTRPA1 (D921N and D925N for chTRPA1; E919Q and E923Q for rsTRPA1) were made, as well as double mutants (D921N/D925N for chTRPA1; E919Q/E923Q for rsTRPA1) and the channel activity of these mutants after heat stimulation in the absence or presence of extracellular Ca^{2+} was examined. Single point mutations in chTRPA1 (D921N and D925N) had inward currents (D921N, green, 48.6 ± 14 pA, $n=6$; D925N, cyan, 44.8 ± 10.4 pA, $n=6$) that were similar to wild type (white, 38.5 ± 7.6 pA, $n=6$) (Fig. 10D and E). A double chTRPA1 mutant (D921N/D925N) showed large inward currents (104 ± 16 pA, $n=6$, navy), which were not affected by the presence of extracellular Ca^{2+} (113 ± 26 pA, $n=6$, pink) and were similar to wild type chTRPA1 currents in the presence of extracellular Ca^{2+} (109.3 ± 22.2 pA, $n=6$, black). For rsTRPA1, the single mutant E919Q (141.6 ± 37.5 pA, $n=5$, green) had similar inward currents in response to heat stimulation compared to wild type (95.1 ± 25.4 pA, $n=6$, white), whereas the E923Q single mutant showed significantly larger heat-evoked currents (189.9 ± 24.9 pA, $n=5$, cyan, $p < 0.05$) than wild type (Fig. 10F and G). Meanwhile, the E919Q/E923Q rsTRPA1 double mutant showed large inward currents (298.4 ± 56.5 pA, $n=5$, navy) that were not affected by extracellular Ca^{2+} (330.2 ± 51.4 pA, $n=5$, pink) and were similar to the wild type rsTRPA1 currents in the presence of extracellular Ca^{2+} (340.3 ± 40.9 pA, $n=7$, black); this pattern was similar to that of chTRPA1. These results suggested that neutralization of the two charged amino acids by extracellular Ca^{2+} is important for the heat-evoked large activation of gaTRPA1, chTRPA1, and rsTRPA1.

Discussion

TRPA1 channels have been primarily reported as cold-activated channels in mice (Story *et al.*, 2003; Bandell *et al.*, 2004), although this phenomenon is a matter of debate (Caspani & Heppenstall, 2009). TRPA1 channel activation by heat stimulation in snakes, frogs, lizards, chicken, *Drosophila*, and mosquitoes was subsequently reported (Wang *et al.*, 2009; Gracheva *et al.*, 2010; Kang *et al.*, 2011; Saito *et al.*, 2012; Saito *et al.*, 2014). Characterization of gaTRPA1 channel properties in a heterologous expression system using HEK293T cells showed that gaTRPA1 was activated by AITC (Fig. 1B), which has been shown to activate mammalian TRPA1 channels (Bandell *et al.*, 2004; Jordt *et al.*, 2004). Mammalian TRPA1s also show desensitization upon repeated chemical stimuli in whole-cell recordings (Raisinghani *et al.*, 2011), a property that is shared by gaTRPA1. However, AITC-induced activation of gaTRPA1 has an EC₅₀ value that is higher than that for the mammalian TRPA1s hTRPA1, rTRPA1 and mTRPA1 (394 μ M vs. 1.9 μ M, 6.2 μ M and 22 μ M, respectively) (Bandell *et al.*, 2004). The outwardly rectifying I-V relationship for AITC-evoked gaTRPA1-mediated currents is also similar to that seen for mammalian TRPA1s (Bandell *et al.*, 2004; Jordt *et al.*, 2004). The temperature sensitivity of gaTRPA1 differed from mammalian TRPA1 in that gaTRPA1 was activated by heat, but not cold stimulus (Fig. 1D) (Story *et al.*, 2003; Bandell *et al.*, 2004). In the absence of AITC, the gaTRPA1 temperature threshold for activation was 35.8 °C (Fig. 3B), which is similar to the value determined in an oocyte system (33.9 °C) (Saito *et al.*, 2012). Notably, both thresholds are slightly higher than the preferred body temperature for green anole lizards (29-30 °C) (Goodman & Walguarnery, 2007), suggesting that gaTRPA1 functions as a noxious heat sensor.

For TRPV1, a heat-gated channel that is also activated by several chemicals, including capsaicin (Caterina *et al.*, 1997), a synergistic activation between chemical and heat

stimulation is well-recognized. However, for mammalian TRPA1 channels, the temperature sensitivity remains unclear. In the present thesis work, a synergism between temperature and chemical sensitivity was clearly apparent in that the AITC sensitivity was increased at higher temperatures that alone did not activate gaTRPA1 (Fig. 3A). Similarly, the temperature threshold for gaTRPA1 activation was decreased with a minimal concentration of AITC that alone could not promote channel activity (Fig. 3C and E). These results indicate that the synergistic properties of gaTRPA1 resemble those of TRPV1. Physiological temperatures were reported to enhance AITC-induced TRPV1 stimulation in mammals (Everaerts *et al.*, 2011), and AITC can directly activate mouse TRPV1 and/or possibly sensitize TRPV1 to heat stimulation in a TRPA1-independent manner (Alpizar *et al.*, 2014). Although there are no reports regarding the function of green anole TRPV1, this channel could be involved in AITC-induced hyperalgesia in green anoles via a mechanism similar to that seen in mammals.

A previous study on cold activation of TRPA1 showed that mTRPA1 is activated by cold in cell-attached patches, but not inside-out patches (Karashima *et al.*, 2009; Chen *et al.*, 2013), suggesting that cold might indirectly activate mTRPA1. Using cell-attached and inside-out patches, another group showed heat-mediated dTRPA1 activation, which may have occurred through a direct mechanism (Wang *et al.*, 2013). The characteristics of the gaTRPA1 single-channel activity (heat- and AITC-sensitivity and I-V relationship) correspond closely with the heat- and AITC-activated currents recorded in a whole-cell configuration. In addition, the observation of both heat- and AITC-evoked single-channel responses in the inside-out configuration indicates a membrane-delimited mechanism for gaTRPA1 activation without involvement of cytosolic factors. As with the whole-cell responses, there are distinct similarities in the characteristics of heat- and AITC-evoked single-channel currents, such as the I-V relationship and mean unitary amplitudes, which indicates that heat and AITC converge to some extent in gaTRPA1 activation.

The functional properties of TRPA1s have been reported for several species. Zebrafish has two paralogous TRPA1 genes (TRPA1a and TRPA1b) (Prober *et al.*, 2008), whereas insects (Coleoptera and Hymenoptera: *B. mori*, *T. castaneum*, *A. mellifera*, *N. vitripennis*) have multiple TRPA subfamily members (Matsuura *et al.*, 2009). As with mammalian TRPA1s, insect TRPA1 channels are activated by noxious chemicals and this sensitivity is further shared with *Drosophila* (Kang *et al.*, 2011). Mammalian TRPA1s have a sensitivity to noxious chemicals that is similar to the gaTRPA1 channel, with conductance for AITC-activated currents of 100 ± 2 pS for hTRPA1 (Komatsu *et al.*, 2012), 73 ± 3 pS for mTRPA1 (Fujita *et al.*, 2008), and 98.4 ± 0.9 pS for gaTRPA1. In terms of heat sensitivity, TRPA1s in insects and some vertebrates such as frogs and snakes are activated by heat, while zebrafish TRPA1 is insensitive to temperature (Prober *et al.*, 2008). Meanwhile, dTRPA1 showed a conductance of 41 ± 2 pS with a linear I-V relationship (Wang *et al.*, 2013), which differs from that seen for gaTRPA1. Although how temperature thresholds for activation of TRPA1 changed from hot to cold is unclear, such changes seem to have occurred at some point in the mammalian evolutionary process, but the chemical sensitivity was preserved.

Interestingly, compared with AITC-activated channels, heat-activated channels produce currents that have shorter open- and closed-times (Fig. 5), suggesting that the two stimuli have different gating mechanisms. For temperature-gating of the TRPA1 channel, the channel opening-closing is obviously complicated as was shown for dTRPA1 (Wang *et al.*, 2013), with sub-conductances more frequently observed than for AITC-activated channels, especially at high membrane potentials. The differences in the open- and closed-times were consistent with the reduction in the dTRPA1 open-time upon heating (Wang *et al.*, 2013). Temperature-dependent changes in open- and closed-time kinetics were also seen for heat-evoked single-channel currents of rTRPV1 (Liu *et al.*, 2003) and heat-evoked single-

channel events in rat DRG neurons that probably involve TRPV1 (Nagy & Rang, 1999). In contrast, Grandl et al. reported that thermal activation of rTRPV1 depends on long channel open times, which were absent in temperature-insensitive mutants (Grandl *et al.*, 2010). Although the precise reason for these differences is unclear, the fact that single channels were analyzed in the range of 10-30 °C may have played a role. The similarity between TRPV1 and TRPA1 suggests that the short durations of channel openings and closings is a common property for heat-gated channel activation.

The roles for Ca^{2+} in heat-evoked TRPA1 channel activation in non-mammalian vertebrates (snakes, frogs and lizards) and *Drosophila* have not been reported, whereas the effects of extracellular and intracellular Ca^{2+} have been studied for mTRPA1. Karashima *et al.* (2009) showed that cold-evoked mTRPA1 activation does not require extracellular/intracellular Ca^{2+} . Our findings showed that heat-evoked activation of gaTRPA1 is dependent on extracellular Ca^{2+} (Fig. 2A), and the fact that even the presence of 1 μM free intracellular Ca^{2+} could not activate the channel upon heat stimulation suggests that extracellular Ca^{2+} , but not intracellular Ca^{2+} , is important for heat-evoked gaTRPA1 activation. On the other hand, both the initial AITC-evoked current sizes and the 2nd/1st current ratios were not dependent on extracellular Ca^{2+} (Fig. 2E and G), which is similar to the mustard oil sensitivity of rTRPA1 in the presence or absence of extracellular Ca^{2+} (Jordt *et al.*, 2004). However, a longer inactivation time (t_{half}) of gaTRPA1 currents induced by AITC stimulation in the absence of extracellular Ca^{2+} (Fig. 2F) suggests that Ca^{2+} influx could accelerate channel inactivation, which is in agreement with earlier results showing that AITC-induced mTRPA1 activation was delayed and slow in the absence of extracellular Ca^{2+} (Nilius *et al.*, 2011).

Heat-evoked activation of gaTRPA1 requires Ca^{2+} binding to negatively charged amino acids near the extracellular face of the channel pore (Fig. 11). Together, extracellular Ca^{2+}

binding and heat could activate the TRPA1 channel, whereas the absence or substitution of other divalent cations for extracellular Ca^{2+} abrogated heat-evoked currents (Fig. 7 A, C and D). The inability of intracellular Ca^{2+} to activate TRPA1 following heat stimulation in our experiments could support our hypothesis that extracellular Ca^{2+} is involved only in heat-evoked activation of gaTRPA1, as opposed to previous reports showing that intracellular Ca^{2+} is important for TRPA1 activation (Jordt *et al.*, 2004; Doerner *et al.*, 2007; Zurborg *et al.*, 2007) as well as potentiation/activation and secondary inactivation after Ca^{2+} influx through the TRPA1 channel following chemical stimulation (Nagata *et al.*, 2005; Karashima *et al.*, 2008; Wang *et al.*, 2008). Meanwhile, heat-evoked activation of chTRPA1 and rsTRPA1 was observed both in the absence and presence of extracellular Ca^{2+} , although the inward currents were significantly smaller in the absence of extracellular Ca^{2+} (Figs. 8 and 9). An alignment of gaTRPA1, chTRPA1, and rsTRPA1 amino acid sequences showed that the residues corresponding to Glu894 in gaTRPA1, 897 and 895, in chTRPA1 and rsTRPA1, respectively, were both Gln (Fig. 9A). Mutation of Glu894 to Gln in the gaTRPA1 channel led to a small, but significant heat-evoked activation even in the absence of extracellular Ca^{2+} , whereas currents for the chTRPA1 (Q897E) and rsTRPA1 (Q895E) mutants were reduced in the absence of extracellular Ca^{2+} (Fig. 9). Moreover, neutralization of acidic amino acids in TRPA1 that are common to all three species may mimic the effect of extracellular Ca^{2+} , since TRPA1 with Gln and Asn showed large heat-evoked inward currents even in the absence of extracellular Ca^{2+} , and the channel sizes were comparable to those seen for wild type channels in the presence of extracellular Ca^{2+} (Fig. 10). Thus, binding of extracellular Ca^{2+} to acidic amino acids is likely important for heat-evoked activation of TRPA1 expressed in green anole, chickens, and rat snakes.

Atomic level structures of TRPV1, a capsaicin- and heat-activated TRP channel, have recently been determined by single-particle analysis with cryo-EM under conditions wherein

the purified protein was in complex with amphipathic polymers or in nanodiscs (Caterina *et al.*, 1997; Cao *et al.*, 2013; Liao *et al.*, 2013; Gao *et al.*, 2016). The structural data suggest that the presence of phosphatidylinositides supports a closed state of TRPV1 and removal of endogenous phosphatidylinositides upon heat stimulation could contribute to channel gating and further cation influx through the TRPV1 pore (Gao *et al.*, 2016). Thus, we propose a new model for extracellular Ca^{2+} -dependent heat-evoked activation of TRPA1 wherein binding of extracellular Ca^{2+} to acidic amino acids near the extracellular side of the TRPA1 channel contributes to channel gating and cation influx upon heat stimulation. Support for this model is provided by the involvement of Glu at position 920 of human TRPA1 in collecting cations into the mouth of the pore and changing the surface potential by ~ 16 mV (Christensen *et al.*, 2016). Our model is also supported by the channel gating and ion permeation of the highly Ca^{2+} -selective channel TRPV6, which involves extracellular cation binding to the channel (Saotome *et al.*, 2016). Although the Ca^{2+} sensitivity and permeability of TRPV6 (>100) (Yue *et al.*, 2001) and TRPA1 (>5) (Karashima *et al.*, 2010) differ, the overall locations of the acidic amino acids in both channels are similar, suggesting that a comparison of the characteristics of the two channels could clarify the significance of Ca^{2+} binding in heat-evoked gating of TRPA1 channels.

Since extracellular Ca^{2+} dependency has not been clearly shown in heat-activated TRPA1 channels from various species (Hamada *et al.*, 2008; Gracheva *et al.*, 2010; Kang *et al.*, 2012; Saito *et al.*, 2012; Saito *et al.*, 2014), we emphasize that, in addition to potentiation/activation or secondary inactivation (Nagata *et al.*, 2005; Karashima *et al.*, 2008; Wang *et al.*, 2008) by intracellular Ca^{2+} , binding of extracellular Ca^{2+} to acidic amino acids in the TRPA1 channel vestibule is important for heat-evoked channel gating. Ca^{2+} concentrations vary in extracellular spaces during development (Brown *et al.*, 1995) and proliferation of various cells such as skin keratinocytes (Pillai *et al.*, 1990), although TRPA1 is not strongly

expressed in epithelial cells. Nonetheless, the dependence of TRPA1 heat-induced activation on extracellular Ca^{2+} in some species could be involved in physiological phenomena that are affected by extracellular Ca^{2+} levels.

In conclusion, I showed similarities and differences between heat and AITC activation of gaTRPA1 in whole-cell and single-channel recordings, which indicates that heat and AITC can directly activate gaTRPA1. I showed the synergistic effects of heat and AITC on gaTRPA1 activation with a reduced temperature threshold for activation in the presence of AITC. I have also identified negatively charged amino acid residues located at the outer vestibule of the gaTRPA1 channel that play an important role in heat-induced channel activation, but do not participate in responses to other stimuli such as AITC. Moreover, the observation that several acidic amino acids in TRPA1 from three species (green anole, chicken, and rat snake) contribute to large channel activation following heat stimuli suggests that allosteric coupling may be involved in this type of channel activation. These findings would be helpful for understanding the mechanisms of TRPA1 activation by temperature.

References

- Alpizar YA, Boonen B, Gees M, Sanchez A, Nilius B, Voets T & Talavera K. (2014). Allyl isothiocyanate sensitizes TRPV1 to heat stimulation. *Pflugers Arch* **466**, 507-515.
- Arnold K, Bordoli L, Kopp J & Schwede T. (2006). The SWISS-MODEL workspace: a web-based environment for protein structure homology modelling. *Bioinformatics* **22**, 195-201.
- Bandell M, Story GM, Hwang SW, Viswanath V, Eid SR, Petrus MJ, Earley TJ & Patapoutian A. (2004). Noxious cold ion channel TRPA1 is activated by pungent compounds and bradykinin. *Neuron* **41**, 849-857.
- Bautista DM, Jordt SE, Nikai T, Tsuruda PR, Read AJ, Poblete J, Yamoah EN, Basbaum AI & Julius D. (2006). TRPA1 mediates the inflammatory actions of environmental irritants and proalgesic agents. *Cell* **124**, 1269-1282.
- Bautista DM, Movahed P, Hinman A, Axelsson HE, Sterner O, Hogestatt ED, Julius D, Jordt SE & Zygmunt PM. (2005). Pungent products from garlic activate the sensory ion channel TRPA1. *Proc Natl Acad Sci U S A* **102**, 12248-12252.
- Bordoli L, Kiefer F, Arnold K, Benkert P, Battey J & Schwede T. (2009). Protein structure homology modeling using SWISS-MODEL workspace. *Nat Protoc* **4**, 1-13.
- Brown EM, Vassilev PM & Hebert SC. (1995). Calcium ions as extracellular messengers. *Cell* **83**, 679-682.
- Caceres AI, Brackmann M, Elia MD, Bessac BF, del Camino D, D'Amours M, Witek JS, Fanger CM, Chong JA, Hayward NJ, Homer RJ, Cohn L, Huang X, Moran MM & Jordt SE. (2009). A sensory neuronal ion channel essential for airway inflammation and hyperreactivity in asthma. *Proc Natl Acad Sci U S A* **106**, 9099-9104.
- Cao E, Liao M, Cheng Y & Julius D. (2013). TRPV1 structures in distinct conformations reveal activation mechanisms. *Nature* **504**, 113-118.
- Caspani O & Heppenstall PA. (2009). TRPA1 and cold transduction: an unresolved issue? *J Gen Physiol* **133**, 245-249.
- Caterina MJ, Rosen TA, Tominaga M, Brake AJ & Julius D. (1999). A capsaicin-receptor homologue with a high threshold for noxious heat. *Nature* **398**, 436-441.

- Caterina MJ, Schumacher MA, Tominaga M, Rosen TA, Levine JD & Julius D. (1997). The capsaicin receptor: a heat-activated ion channel in the pain pathway. *Nature* **389**, 816-824.
- Chen J, Joshi SK, DiDomenico S, Perner RJ, Mikusa JP, Gauvin DM, Segreti JA, Han P, Zhang XF, Niforatos W, Bianchi BR, Baker SJ, Zhong C, Simler GH, McDonald HA, Schmidt RG, McGaraughty SP, Chu KL, Faltynek CR, Kort ME, Reilly RM & Kym PR. (2011). Selective blockade of TRPA1 channel attenuates pathological pain without altering noxious cold sensation or body temperature regulation. *Pain* **152**, 1165-1172.
- Chen J, Kang D, Xu J, Lake M, Hogan JO, Sun C, Walter K, Yao B & Kim D. (2013). Species differences and molecular determinant of TRPA1 cold sensitivity. *Nat Commun* **4**, 2501.
- Christensen AP, Akyuz N & Corey DP. (2016). The Outer Pore and Selectivity Filter of TRPA1. *PLoS One* **11**, e0166167.
- Clapham DE & Miller C. (2011). A thermodynamic framework for understanding temperature sensing by transient receptor potential (TRP) channels. *Proc Natl Acad Sci U S A* **108**, 19492-19497.
- Cordero-Morales JF, Gracheva EO & Julius D. (2011). Cytoplasmic ankyrin repeats of transient receptor potential A1 (TRPA1) dictate sensitivity to thermal and chemical stimuli. *Proc Natl Acad Sci U S A* **108**, E1184-1191.
- Doerner JF, Gisselmann G, Hatt H & Wetzel CH. (2007). Transient receptor potential channel A1 is directly gated by calcium ions. *J Biol Chem* **282**, 13180-13189.
- Eid SR, Crown ED, Moore EL, Liang HA, Choong KC, Dima S, Henze DA, Kane SA & Urban MO. (2008). HC-030031, a TRPA1 selective antagonist, attenuates inflammatory- and neuropathy-induced mechanical hypersensitivity. *Mol Pain* **4**, 48.
- Everaerts W, Gees M, Alpizar YA, Farre R, Leten C, Apetrei A, Dewachter I, van Leuven F, Vennekens R, De Ridder D, Nilius B, Voets T & Talavera K. (2011). The capsaicin receptor TRPV1 is a crucial mediator of the noxious effects of mustard oil. *Curr Biol* **21**, 316-321.
- Fujita F, Uchida K, Moriyama T, Shima A, Shibasaki K, Inada H, Sokabe T & Tominaga M. (2008). Intracellular alkalization causes pain sensation through activation of TRPA1 in mice. *J Clin Invest* **118**, 4049-4057.

- Gao Y, Cao E, Julius D & Cheng Y. (2016). TRPV1 structures in nanodiscs reveal mechanisms of ligand and lipid action. *Nature* **534**, 347-351.
- Gaudet R. (2008). TRP channels entering the structural era. *J Physiol* **586**, 3565-3575.
- Goodman RM & Walguarnery JW. (2007). Incubation temperature modifies neonatal thermoregulation in the lizard *Anolis carolinensis*. *J Exp Zool A Ecol Genet Physiol* **307**, 439-448.
- Gracheva EO, Ingolia NT, Kelly YM, Cordero-Morales JF, Hollopeter G, Chesler AT, Sanchez EE, Perez JC, Weissman JS & Julius D. (2010). Molecular basis of infrared detection by snakes. *Nature* **464**, 1006-1011.
- Grandl J, Kim SE, Uzzell V, Bursulaya B, Petrus M, Bandell M & Patapoutian A. (2010). Temperature-induced opening of TRPV1 ion channel is stabilized by the pore domain. *Nat Neurosci* **13**, 708-714.
- Guler AD, Lee H, Iida T, Shimizu I, Tominaga M & Caterina M. (2002). Heat-evoked activation of the ion channel, TRPV4. *J Neurosci* **22**, 6408-6414.
- Gupta R, Saito S, Mori Y, Itoh SG, Okumura H & Tominaga M. (2016). Structural basis of TRPA1 inhibition by HC-030031 utilizing species-specific differences. *Sci Rep* **6**, 37460.
- Hamada FN, Rosenzweig M, Kang K, Pulver SR, Ghezzi A, Jegla TJ & Garrity PA. (2008). An internal thermal sensor controlling temperature preference in *Drosophila*. *Nature* **454**, 217-220.
- Hinman A, Chuang HH, Bautista DM & Julius D. (2006). TRP channel activation by reversible covalent modification. *Proc Natl Acad Sci U S A* **103**, 19564-19568.
- Iwasaki Y, Tanabe M, Kayama Y, Abe M, Kashio M, Koizumi K, Okumura Y, Morimitsu Y, Tominaga M, Ozawa Y & Watanabe T. (2009). Miogadial and miogatrial with alpha,beta-unsaturated 1,4-dialdehyde moieties--novel and potent TRPA1 agonists. *Life Sci* **85**, 60-69.
- Jaquemar D, Schenker T & Trueb B. (1999). An ankyrin-like protein with transmembrane domains is specifically lost after oncogenic transformation of human fibroblasts. *J Biol Chem* **274**, 7325-7333.
- Jara-Oseguera A & Islas LD. (2013). The role of allosteric coupling on thermal activation of thermo-TRP channels. *Biophys J* **104**, 2160-2169.

- Jordt SE, Bautista DM, Chuang HH, McKemy DD, Zygmunt PM, Hogestatt ED, Meng ID & Julius D. (2004). Mustard oils and cannabinoids excite sensory nerve fibres through the TRP channel ANKTM1. *Nature* **427**, 260-265.
- Kang K, Panzano VC, Chang EC, Ni L, Dainis AM, Jenkins AM, Regna K, Muskavitch MA & Garrity PA. (2011). Modulation of TRPA1 thermal sensitivity enables sensory discrimination in *Drosophila*. *Nature* **481**, 76-80.
- Kang K, Panzano VC, Chang EC, Ni L, Dainis AM, Jenkins AM, Regna K, Muskavitch MA & Garrity PA. (2012). Modulation of TRPA1 thermal sensitivity enables sensory discrimination in *Drosophila*. *Nature* **481**, 76-80.
- Karashima Y, Prenen J, Meseguer V, Owsianik G, Voets T & Nilius B. (2008). Modulation of the transient receptor potential channel TRPA1 by phosphatidylinositol 4,5-bisphosphate manipulators. *Pflugers Arch* **457**, 77-89.
- Karashima Y, Prenen J, Talavera K, Janssens A, Voets T & Nilius B. (2010). Agonist-induced changes in Ca(2+) permeation through the nociceptor cation channel TRPA1. *Biophys J* **98**, 773-783.
- Karashima Y, Talavera K, Everaerts W, Janssens A, Kwan KY, Vennekens R, Nilius B & Voets T. (2009). TRPA1 acts as a cold sensor in vitro and in vivo. *Proc Natl Acad Sci U S A* **106**, 1273-1278.
- Kashio M, Sokabe T, Shintaku K, Uematsu T, Fukuta N, Kobayashi N, Mori Y & Tominaga M. (2012). Redox signal-mediated sensitization of transient receptor potential melastatin 2 (TRPM2) to temperature affects macrophage functions. *Proc Natl Acad Sci U S A* **109**, 6745-6750.
- Kiefer F, Arnold K, Kunzli M, Bordoli L & Schwede T. (2009). The SWISS-MODEL Repository and associated resources. *Nucleic Acids Res* **37**, D387-392.
- Kohno K, Sokabe T, Tominaga M & Kadowaki T. (2010). Honey bee thermal/chemical sensor, AmHsTRPA, reveals neofunctionalization and loss of transient receptor potential channel genes. *J Neurosci* **30**, 12219-12229.
- Komatsu T, Uchida K, Fujita F, Zhou Y & Tominaga M. (2012). Primary alcohols activate human TRPA1 channel in a carbon chain length-dependent manner. *Pflugers Arch* **463**, 549-559.

- Koo JY, Jang Y, Cho H, Lee CH, Jang KH, Chang YH, Shin J & Oh U. (2007). Hydroxy-alpha-sanshool activates TRPV1 and TRPA1 in sensory neurons. *Eur J Neurosci* **26**, 1139-1147.
- Kremeyer B, Lopera F, Cox JJ, Momin A, Rugiero F, Marsh S, Woods CG, Jones NG, Paterson KJ, Fricker FR, Villegas A, Acosta N, Pineda-Trujillo NG, Ramirez JD, Zea J, Burley MW, Bedoya G, Bennett DL, Wood JN & Ruiz-Linares A. (2010). A gain-of-function mutation in TRPA1 causes familial episodic pain syndrome. *Neuron* **66**, 671-680.
- Kurganov E, Zhou Y, Saito S & Tominaga M. (2014). Heat and AITC activate green anole TRPA1 in a membrane-delimited manner. *Pflugers Arch* **466**, 1873-1884.
- Kwan KY, Allchorne AJ, Vollrath MA, Christensen AP, Zhang DS, Woolf CJ & Corey DP. (2006). TRPA1 contributes to cold, mechanical, and chemical nociception but is not essential for hair-cell transduction. *Neuron* **50**, 277-289.
- Laursen WJ, Anderson EO, Hoffstaetter LJ, Bagriantsev SN & Gracheva EO. (2015). Species-specific temperature sensitivity of TRPA1. *Temperature (Austin)* **2**, 214-226.
- Liao M, Cao E, Julius D & Cheng Y. (2013). Structure of the TRPV1 ion channel determined by electron cryo-microscopy. *Nature* **504**, 107-112.
- Liu B, Hui K & Qin F. (2003). Thermodynamics of heat activation of single capsaicin ion channels VR1. *Biophys J* **85**, 2988-3006.
- Liu C & Zwiebel LJ. (2013). Molecular characterization of larval peripheral thermosensory responses of the malaria vector mosquito *Anopheles gambiae*. *PLoS One* **8**, e72595.
- Macpherson LJ, Dubin AE, Evans MJ, Marr F, Schultz PG, Cravatt BF & Patapoutian A. (2007). Noxious compounds activate TRPA1 ion channels through covalent modification of cysteines. *Nature* **445**, 541-545.
- Macpherson LJ, Geierstanger BH, Viswanath V, Bandell M, Eid SR, Hwang S & Patapoutian A. (2005). The pungency of garlic: activation of TRPA1 and TRPV1 in response to allicin. *Curr Biol* **15**, 929-934.
- Matsuura H, Sokabe T, Kohno K, Tominaga M & Kadowaki T. (2009). Evolutionary conservation and changes in insect TRP channels. *BMC Evol Biol* **9**, 228.

- McHugh D, Flemming R, Xu SZ, Perraud AL & Beech DJ. (2003). Critical intracellular Ca²⁺ dependence of transient receptor potential melastatin 2 (TRPM2) cation channel activation. *J Biol Chem* **278**, 11002-11006.
- McKemy DD, Neuhauser WM & Julius D. (2002). Identification of a cold receptor reveals a general role for TRP channels in thermosensation. *Nature* **416**, 52-58.
- McNamara CR, Mandel-Brehm J, Bautista DM, Siemens J, Deranian KL, Zhao M, Hayward NJ, Chong JA, Julius D, Moran MM & Fanger CM. (2007). TRPA1 mediates formalin-induced pain. *Proc Natl Acad Sci U S A* **104**, 13525-13530.
- Moparthy L, Kichko TI, Eberhardt M, Hogestatt ED, Kjellbom P, Johanson U, Reeh PW, Leffler A, Filipovic MR & Zygmunt PM. (2016). Human TRPA1 is a heat sensor displaying intrinsic U-shaped thermosensitivity. *Sci Rep* **6**, 28763.
- Moparthy L, Survery S, Kreir M, Simonsen C, Kjellbom P, Hogestatt ED, Johanson U & Zygmunt PM. (2014). Human TRPA1 is intrinsically cold- and chemosensitive with and without its N-terminal ankyrin repeat domain. *Proc Natl Acad Sci U S A* **111**, 16901-16906.
- Nagata K, Duggan A, Kumar G & Garcia-Anoveros J. (2005). Nociceptor and hair cell transducer properties of TRPA1, a channel for pain and hearing. *J Neurosci* **25**, 4052-4061.
- Nagy I & Rang HP. (1999). Similarities and differences between the responses of rat sensory neurons to noxious heat and capsaicin. *J Neurosci* **19**, 10647-10655.
- Nilius B, Mahieu F, Prenen J, Janssens A, Owsianik G, Vennekens R & Voets T. (2006). The Ca²⁺-activated cation channel TRPM4 is regulated by phosphatidylinositol 4,5-bisphosphate. *EMBO J* **25**, 467-478.
- Nilius B, Prenen J & Owsianik G. (2011). Irritating channels: the case of TRPA1. *J Physiol* **589**, 1543-1549.
- Okumura Y, Narukawa M, Iwasaki Y, Ishikawa A, Matsuda H, Yoshikawa M & Watanabe T. (2010). Activation of TRPV1 and TRPA1 by black pepper components. *Biosci Biotechnol Biochem* **74**, 1068-1072.
- Paulsen CE, Armache JP, Gao Y, Cheng Y & Julius D. (2015). Structure of the TRPA1 ion channel suggests regulatory mechanisms. *Nature* **520**, 511-517.

- Peier AM, Moqrich A, Hergarden AC, Reeve AJ, Andersson DA, Story GM, Earley TJ, Dragoni I, McIntyre P, Bevan S & Patapoutian A. (2002a). A TRP channel that senses cold stimuli and menthol. *Cell* **108**, 705-715.
- Peier AM, Reeve AJ, Andersson DA, Moqrich A, Earley TJ, Hergarden AC, Story GM, Colley S, Hogenesch JB, McIntyre P, Bevan S & Patapoutian A. (2002b). A heat-sensitive TRP channel expressed in keratinocytes. *Science* **296**, 2046-2049.
- Petrus M, Peier AM, Bandell M, Hwang SW, Huynh T, Olney N, Jegla T & Patapoutian A. (2007). A role of TRPA1 in mechanical hyperalgesia is revealed by pharmacological inhibition. *Mol Pain* **3**, 40.
- Peyrot des Gachons C, Uchida K, Bryant B, Shima A, Sperry JB, Dankulich-Nagrudny L, Tominaga M, Smith AB, 3rd, Beauchamp GK & Breslin PA. (2011). Unusual pungency from extra-virgin olive oil is attributable to restricted spatial expression of the receptor of oleocanthal. *J Neurosci* **31**, 999-1009.
- Pillai S, Bickle DD, Mancianti ML, Cline P & Hincenbergs M. (1990). Calcium regulation of growth and differentiation of normal human keratinocytes: modulation of differentiation competence by stages of growth and extracellular calcium. *J Cell Physiol* **143**, 294-302.
- Prober DA, Zimmerman S, Myers BR, McDermott BM, Jr., Kim SH, Caron S, Rihel J, Solnica-Krezel L, Julius D, Hudspeth AJ & Schier AF. (2008). Zebrafish TRPA1 channels are required for chemosensation but not for thermosensation or mechanosensory hair cell function. *J Neurosci* **28**, 10102-10110.
- Qin F. (2013). Demystifying thermal channels: driving a channel both forwards and backwards with a single gear? *Biophys J* **104**, 2118-2120.
- Raisinghani M, Zhong L, Jeffry JA, Bishnoi M, Pabbidi RM, Pimentel F, Cao DS, Evans MS & Premkumar LS. (2011). Activation characteristics of transient receptor potential ankyrin 1 and its role in nociception. *Am J Physiol Cell Physiol* **301**, C587-600.
- Saito S, Banzawa N, Fukuta N, Saito CT, Takahashi K, Imagawa T, Ohta T & Tominaga M. (2014). Heat and noxious chemical sensor, chicken TRPA1, as a target of bird repellents and identification of its structural determinants by multispecies functional comparison. *Mol Biol Evol* **31**, 708-722.
- Saito S, Nakatsuka K, Takahashi K, Fukuta N, Imagawa T, Ohta T & Tominaga M. (2012). Analysis of transient receptor potential ankyrin 1 (TRPA1) in frogs and lizards illuminates both nociceptive heat and chemical sensitivities and coexpression with TRP vanilloid 1 (TRPV1) in ancestral vertebrates. *J Biol Chem* **287**, 30743-30754.

- Saito S & Tominaga M. (2015). Functional diversity and evolutionary dynamics of thermoTRP channels. *Cell Calcium* **57**, 214-221.
- Salazar M, Moldenhauer H & Baez-Nieto D. (2011). Could an allosteric gating model explain the role of TRPA1 in cold hypersensitivity? *J Neurosci* **31**, 5554-5556.
- Saotome K, Singh AK, Yelshanskaya MV & Sobolevsky AI. (2016). Crystal structure of the epithelial calcium channel TRPV6. *Nature* **534**, 506-511.
- Sato A, Sokabe T, Kashio M, Yasukochi Y, Tominaga M & Shiomi K. (2014). Embryonic thermosensitive TRPA1 determines transgenerational diapause phenotype of the silkworm, *Bombyx mori*. *Proc Natl Acad Sci U S A* **111**, E1249-1255.
- Smith GD, Gunthorpe MJ, Kelsell RE, Hayes PD, Reilly P, Facer P, Wright JE, Jerman JC, Walhin JP, Ooi L, Egerton J, Charles KJ, Smart D, Randall AD, Anand P & Davis JB. (2002). TRPV3 is a temperature-sensitive vanilloid receptor-like protein. *Nature* **418**, 186-190.
- Story GM, Peier AM, Reeve AJ, Eid SR, Mosbacher J, Hricik TR, Earley TJ, Hergarden AC, Andersson DA, Hwang SW, McIntyre P, Jegla T, Bevan S & Patapoutian A. (2003). ANKTM1, a TRP-like channel expressed in nociceptive neurons, is activated by cold temperatures. *Cell* **112**, 819-829.
- Takaishi M, Fujita F, Uchida K, Yamamoto S, Sawada Shimizu M, Hatai Uotsu C, Shimizu M & Tominaga M. (2012). 1,8-cineole, a TRPM8 agonist, is a novel natural antagonist of human TRPA1. *Mol Pain* **8**, 86.
- Takaishi M, Uchida K, Fujita F & Tominaga M. (2014). Inhibitory effects of monoterpenes on human TRPA1 and the structural basis of their activity. *J Physiol Sci* **64**, 47-57.
- Talavera K, Yasumatsu K, Voets T, Droogmans G, Shigemura N, Ninomiya Y, Margolskee RF & Nilius B. (2005). Heat activation of TRPM5 underlies thermal sensitivity of sweet taste. *Nature* **438**, 1022-1025.
- Togashi K, Hara Y, Tominaga T, Higashi T, Konishi Y, Mori Y & Tominaga M. (2006). TRPM2 activation by cyclic ADP-ribose at body temperature is involved in insulin secretion. *EMBO J* **25**, 1804-1815.
- Viswanath V, Story GM, Peier AM, Petrus MJ, Lee VM, Hwang SW, Patapoutian A & Jegla T. (2003). Opposite thermosensor in fruitfly and mouse. *Nature* **423**, 822-823.

- Voets T. (2012). Quantifying and modeling the temperature-dependent gating of TRP channels. *Rev Physiol Biochem Pharmacol* **162**, 91-119.
- Voets T, Droogmans G, Wissenbach U, Janssens A, Flockerzi V & Nilius B. (2004). The principle of temperature-dependent gating in cold- and heat-sensitive TRP channels. *Nature* **430**, 748-754.
- Vriens J, Owsianik G, Hofmann T, Philipp SE, Stab J, Chen X, Benoit M, Xue F, Janssens A, Kerselaers S, Oberwinkler J, Vennekens R, Gudermann T, Nilius B & Voets T. (2011). TRPM3 is a nociceptor channel involved in the detection of noxious heat. *Neuron* **70**, 482-494.
- Wang G, Qiu YT, Lu T, Kwon HW, Pitts RJ, Van Loon JJ, Takken W & Zwiebel LJ. (2009). *Anopheles gambiae* TRPA1 is a heat-activated channel expressed in thermosensitive sensilla of female antennae. *Eur J Neurosci* **30**, 967-974.
- Wang H, Schupp M, Zurborg S & Heppenstall PA. (2013). Residues in the pore region of *Drosophila* transient receptor potential A1 dictate sensitivity to thermal stimuli. *J Physiol* **591**, 185-201.
- Wang YY, Chang RB, Waters HN, McKemy DD & Liman ER. (2008). The nociceptor ion channel TRPA1 is potentiated and inactivated by permeating calcium ions. *J Biol Chem* **283**, 32691-32703.
- Wei H, Hamalainen MM, Saarnilehto M, Koivisto A & Pertovaara A. (2009). Attenuation of mechanical hypersensitivity by an antagonist of the TRPA1 ion channel in diabetic animals. *Anesthesiology* **111**, 147-154.
- Wu LJ, Sweet TB & Clapham DE. (2010). International Union of Basic and Clinical Pharmacology. LXXVI. Current progress in the mammalian TRP ion channel family. *Pharmacol Rev* **62**, 381-404.
- Xiao R, Tang J, Wang C, Colton CK, Tian J & Zhu MX. (2008). Calcium plays a central role in the sensitization of TRPV3 channel to repetitive stimulations. *J Biol Chem* **283**, 6162-6174.
- Xu H, Ramsey IS, Kotecha SA, Moran MM, Chong JA, Lawson D, Ge P, Lilly J, Silos-Santiago I, Xie Y, DiStefano PS, Curtis R & Clapham DE. (2002). TRPV3 is a calcium-permeable temperature-sensitive cation channel. *Nature* **418**, 181-186.
- Yue L, Peng JB, Hediger MA & Clapham DE. (2001). CaT1 manifests the pore properties of the calcium-release-activated calcium channel. *Nature* **410**, 705-709.

Zhang XF, Chen J, Faltynek CR, Moreland RB & Neelands TR. (2008). Transient receptor potential A1 mediates an osmotically activated ion channel. *Eur J Neurosci* **27**, 605-611.

Zimmermann K, Lennerz JK, Hein A, Link AS, Kaczmarek JS, Delling M, Uysal S, Pfeifer JD, Riccio A & Clapham DE. (2011). Transient receptor potential cation channel, subfamily C, member 5 (TRPC5) is a cold-transducer in the peripheral nervous system. *Proc Natl Acad Sci U S A* **108**, 18114-18119.

Zurborg S, Yurgionas B, Jira JA, Caspani O & Heppenstall PA. (2007). Direct activation of the ion channel TRPA1 by Ca^{2+} . *Nat Neurosci* **10**, 277-279.

Figure legends

Figure 1

Heat and AITC sensitivities of green anole TRPA1 expressed in HEK 293 cells

A and B, Representative current (upper) and temperature (lower) traces for repeated heat and AITC stimulation in HEK293 cells expressing green anole TRPA1. **C**, Representative gaTRPA1-mediated whole-cell current traces upon application of heat and AITC (400 μ M) recorded at -60 mV with voltage-ramp pulses (-100 to +100 mV in 500 ms) every 5 s. Current-voltage relationships of heat- and AITC-evoked responses are shown (**C**, inset). **D**, Representative current (upper) and temperature (lower) traces for repeated cold, heat and AITC stimulation.

Figure 2

Comparison of heat- and AITC-evoked currents in the presence and absence of extracellular Ca^{2+}

A, Representative current (upper) and temperature (lower) traces for heat and AITC stimulation in the absence of extracellular Ca^{2+} . **B**, The average difference in heat-evoked gaTRPA1 currents in the presence (filled) and absence (open) of extracellular Ca^{2+} . **C**, Representative gaTRPA1-mediated whole-cell current traces upon application of heat and AITC (400 μ M) recorded at -60 mV with voltage-ramp pulses (-100 to +100 mV in 500 ms) every 5 s in the absence of extracellular Ca^{2+} . Current-voltage relationships for heat- and AITC-evoked gaTRPA1 currents are shown (**C**, inset). **D**, Representative current traces for repeated AITC stimulation in the absence of extracellular Ca^{2+} . **E**, Comparison of initial AITC-evoked currents in the presence (filled) and absence (open) of extracellular Ca^{2+} . **F**,

Comparison of t_{half} (time for half inactivation) of the initial AITC-evoked currents in the presence (filled) and absence (open) of extracellular Ca^{2+} . **G**, Comparison of the 2nd/1st ratio of AITC-evoked currents in the presence (filled) and absence (open) of extracellular Ca^{2+} . Data represent the mean \pm S.E.M. (n=6-8). ** $p < 0.01$.

Figure 3

Synergistic effects of heat and AITC on gaTRPA1 activation

A, Dose-response curves for gaTRPA1 current responses to AITC at 25 °C (black line) and 30 °C (red line). Data are shown as the mean \pm S.E.M. (n = 6-13). **B - D**, Arrhenius plot of the currents elicited by heat stimulation at 15-18 °C (**B** and **C**) or 25 °C (**D**) without AITC (**B** and **D**) or with 20 μM AITC treatment for 1 min (**C**). The average temperature thresholds for heat stimulation were 35.8 ± 0.5 °C (n=6; **B**), 26.9 ± 0.8 °C (n = 6; **C**) and 36.4 ± 0.5 °C (n=7; **D**). Representative current traces upon application of heat at 15-18 °C without (**B**, inset) and with AITC (**C**, inset), and at 25 °C without AITC (**D**, inset). **E**, The average difference in temperature thresholds for gaTRPA1 activation expressed in HEK293 cells without or with AITC from different basal temperatures. – and + represent the absence and presence of AITC, respectively. Data represent the mean \pm S.E.M. (n=6). ** $p < 0.01$.

Figure 4

Single-channel currents of green anole TRPA1 in HEK293 cells activated by heat or AITC

A and **B**, Representative single-channel current traces obtained in inside-out patches excised from HEK293 cells expressing gaTRPA1 at $V_p = -60$ mV. Temperature changes are also shown in **A**. *Insets* 1, 2, and 3 show the indicated segments of the continued current traces with expanded scales and real temperatures in **A**. The dotted lines indicate closed (c) and open (o) levels. **C** and **D**, Recordings of heat- and AITC-induced single-channel events at different membrane potentials in an inside-out patch configuration. The dotted lines indicate closed (c) and open (o) levels. **E** and **F**, The single-channel I-V curves of heat- and AITC-activated channels in inside-out patches ($n = 6$). Both curves show outward rectification. Data represent the mean \pm S.D. ($n = 6$).

Figure 5

Comparison of single-channel properties produced by heat and AITC recorded in inside-out patches at +60 mV

A and **B**, Single-channel events induced by heat and AITC. **C**- **E**, open-time distribution of channel openings induced by heat (**C**) and AITC (**D**) and time difference in open-times between heat and AITC (**e**). **F** - **H**, closed-time distribution of channel openings induced by heat (**F**) and AITC (**G**) and time difference in closed-times between heat and AITC (**H**). Data represent the mean \pm S.E.M. ($n = 6$).

Figure 6

Comparison of single-channel properties produced by AITC recorded in inside-out patches at +60 mV in the presence and absence of extracellular Ca²⁺

A, Representative single-channel current traces obtained in inside-out patches excised from HEK293 cells expressing gaTRPA1 at $V_p = -60$ mV in the absence of extracellular Ca²⁺. *Insets* 1, 2 and 3 show the indicated segments of the continued current traces with expanded scales. The dotted lines indicate closed (c) and open (o) levels. **B** and **C**, Amplitude histogram of channel events in the absence of extracellular Ca²⁺ (**B**) and comparison between the presence and absence of extracellular Ca²⁺ (**C**). Unitary amplitudes for currents activated by AITC in the presence and absence of extracellular Ca²⁺ were 4.2 ± 0.1 pA and 4.13 ± 0.27 pA, respectively. **D** and **E**, Open-time distribution of channel openings induced by AITC in the absence of extracellular Ca²⁺ (**D**) and time difference in open-times between the presence and absence of extracellular Ca²⁺ (**E**). **F** and **G**, Closed-time distribution of channel openings induced by AITC in the absence of extracellular Ca²⁺ (**F**) and time difference in closed-times between the presence and absence of extracellular Ca²⁺ (**G**). Data represent the mean \pm S.E.M. (n = 6).

Figure 7

Heat-evoked gaTRPA1 currents in HEK293T cells in the absence and presence of extracellular Ca²⁺

A, Representative current (upper) and temperature (lower) traces in response to heat or AITC (400 μ M) stimulation in the absence of extracellular Ca²⁺ in HEK293T cells expressing gaTRPA1. HC030031 (50 μ M) was added after AITC stimulation. The pipette solution included 1 μ M intracellular free Ca²⁺. **B**, Representative current (upper) and temperature

(lower) traces for heat and AITC (400 μM) stimulation in the absence of extracellular and intracellular Ca^{2+} . **C**, Representative current (upper) and temperature (lower) traces in the absence of extracellular Mg^{2+} with extracellular Ca^{2+} (2 mM) in HEK293T cells expressing gaTRPA1. **D**, Representative current (upper) and temperature (lower) traces in response to heat or AITC (400 μM) stimulation in the presence of extracellular Ba^{2+} (2 mM) and absence of extracellular Ca^{2+} in HEK293T cells expressing gaTRPA1. **E**, Representative gaTRPA1-mediated heat-evoked whole-cell current traces. Lines above the traces show heat stimulation duration. Extracellular Ca^{2+} concentrations ($[\text{Ca}^{2+}]_o$) are shown below the traces. **F**, Heat-evoked gaTRPA1 current densities at different extracellular Ca^{2+} concentrations. **G** and **H**, Representative current (upper) and temperature (lower) traces for gaTRPA1 and Arrhenius plots of currents elicited by heat stimulation at 25 $^{\circ}\text{C}$ at 1 mM (**G**) and 2 mM (**H**) extracellular Ca^{2+} . The average temperature thresholds for activation by heat were 34.9 ± 1.9 $^{\circ}\text{C}$, ($n=4$; **G**) and 35.8 ± 1.8 $^{\circ}\text{C}$, ($n=6$; **H**) at 1 mM and 2 mM extracellular Ca^{2+} , respectively **I**, Temperature thresholds for heat-induced gaTRPA1 activation at 1 mM and 2 mM extracellular Ca^{2+} . Holding potential was -60 mV. Data represent the mean \pm S.E.M. ($n=5-8$). * $p < 0.05$ vs. 0 mM; # $p < 0.05$ vs. 2 mM.

Figure 8

Heat-evoked currents of chTRPA1 and rsTRPA1 expressed in HEK293T cells in the presence and absence of extracellular Ca^{2+}

A and **B**, Representative current (upper) and temperature (lower) traces for chTRPA1 in the presence (**A**) and absence (**B**) of extracellular Ca^{2+} . **C**, Arrhenius plots of currents elicited by heat stimulation from 25 $^{\circ}\text{C}$ in the presence (left) and absence (right) of extracellular Ca^{2+} . The average temperature thresholds for heat-evoked activation were 39.3 ± 0.5 $^{\circ}\text{C}$, ($n=5$) and 39.6 ± 1.2 $^{\circ}\text{C}$ ($n=6$) in the presence and absence of extracellular Ca^{2+} , respectively. **D**,

Temperature thresholds for chTRPA1 activation at 2 mM (filled) and 0 mM (blank) extracellular Ca^{2+} . Data represent the mean \pm S.E.M. ($n=5$). n.s. – no significance. **E** and **F**, Representative current (upper) and temperature (lower) traces for rsTRPA1 in the presence (E) and absence (F) of extracellular Ca^{2+} . **G**, Arrhenius plots of currents elicited by heat stimulation from 25 °C in the presence (left) and absence (right) of extracellular Ca^{2+} . Temperature thresholds for heat-evoked activation were 37.4 ± 0.9 °C ($n=6$) and 39 ± 0.6 °C ($n=6$) in the presence and absence of extracellular Ca^{2+} . **H**, Temperature thresholds for rsTRPA1 activation at 2 mM (filled) and 0 mM (blank) extracellular Ca^{2+} . Data represent the mean \pm S.E.M. ($n=6$). n.s. – no significance.

Figure 9

Location of gaTRPA1 amino acid residues that is required for heat-evoked activation

A, Alignment of TM5 amino acids in gaTRPA1, chTRPA1, and rsTRPA1. The location of amino acids that differ from gaTRPA1 (E894) is indicated in red. Numbering is based on the gaTRPA1 sequence. *-identical, :-similar, .-different. **B**, A side view of the homology model structure for two gaTRPA1 subunits based on hTRPA1. The red and black arrow indicate the E894 side chain and direction of ion flow, respectively. **C** and **D**, Representative current (upper) and temperature (lower) traces for gaTRPA1 (E894Q) in the presence (C) and absence (D) of extracellular Ca^{2+} . **E**, Comparison of AITC-evoked currents for wild type (black) and E894Q (grey and white) gaTRPA1 in the presence and absence of extracellular Ca^{2+} . **F**, Representative current (upper) and temperature (lower) traces for heat and AITC (400 μM) stimulation in the absence of extracellular and intracellular Ca^{2+} in HEK293T cells expressing gaTRPA1 mutant (E894K). **G**, Representative current (upper) and temperature (lower) traces for heat stimulation in the presence of extracellular and absence of intracellular Ca^{2+} in HEK293T cells expressing gaTRPA1 mutant (E894K). **H**, **I**, **K** and **L**, Representative

current (upper) and temperature (lower) traces for chTRPA1 (Q897E) (**H, I**) and rsTRPA1 (Q895E) (**K, L**) in the presence (**H, IK**) and absence (**I, L**) of extracellular Ca^{2+} . **J** and **M**, Comparison of heat-evoked currents for wild type (black and white) and Q to E mutants (light and dark grey) of chTRPA1 (**J**) and rsTRPA1 (**M**) in the presence (+) and absence (-) of extracellular Ca^{2+} . Data represent the mean \pm S.E.M. (n=4-6). n.s., no significance; * $p < 0.05$ vs WT (+ and -), Q897E and Q895E (+); # $p < 0.05$ vs WT (+), Q897E and Q895E (+).

Figure 10

Heat-evoked activation of wild type and mutant TRPA1 channels from three species.

A, Amino acid sequence alignment of gaTRPA1, chTRPA1, and rsTRPA1. The locations of TM5, pore helix 1, pore helix 2, and TM6 are indicated by lines above the alignment. The negatively charged amino acids examined are shown in red (gaTRPA1), green, and cyan (all three species). Numbering on the right of the alignment is based on gaTRPA1. *-identical, :-similar, .-different. *-identical, :-similar, .-different. **B, D** and **F**, Representative heat-evoked whole-cell current traces recorded at -60 mV for gaTRPA1 (**B**), chTRPA1 (**D**), and rsTRPA1 (**F**) having the indicated mutations. **C, E** and **G**, Comparison of heat-evoked activation of wild type and mutated gaTRPA1 channels (**C**), chTRPA1 (**E**) and rsTRPA1 (**G**) in the presence and absence (*minus sign*) of extracellular Ca^{2+} . Data represent the mean \pm S.E.M. (n=5-7). n.s. – no significance. * $p < 0.05$ vs WT (+). # $p < 0.05$ vs E894Q/D918N/E922Q (-,-,+); D921N/D925N (-,+); E919Q/E923Q (-,+). † $p < 0.05$ vs. E894Q; E894Q/D918N; E894Q/E922Q (-). ‡ $p < 0.05$ vs WT (-).

Figure 11

Possible external Ca^{2+} binding sites on the gaTRPA1 channel. A ribbon representation showing a side view of the transmembrane domains of two opposing gaTRPA1 model subunits based on hTRPA1 is shown. The side chains of mutated amino acids are indicated by red arrows and the black downward vertical arrow indicates the direction of ion flow.

Table and Figures

Table 1

Primer sets for green anole, chicken and rat snake TRPA1 glutamate/glutamine, glutamine/glutamate, aspartate/asparagine and glutamate/lysine mutations

Green anole TRPA1	Sense primer (5'→3')	Antisense primer (5'→3')
E894Q	CTTCTTGGTTCACAGcAAGCATATGGCACTCC	GGAGTGCCATATGCTTgCTGTGAACCAAGAAG
E894K	TCACAGaAAGCATATGGCACTC	CATATGCTTtCTGTGAACCAAGAAG
D918N	GATATCAATTATCATaATGCTTTCCCTTGA	TCAAGGAAAGCATtATGATAATTGATATC
E922Q	CATGATGCTTTCCTTcAACCAATGTTGAC	GTC AACATTGGTTgAAGGAAAGCATCATG
E922Q (D918N)	CATaATGCTTTCCTTcAACCAATGTTGAC	GTC AACATTGGTTgAAGGAAAGCATtATG
Chicken TRPA1	Sense primer (5'→3')	Antisense primer (5'→3')
Q897E	CCTTTTGGGTTACACAGgAAACATACAGCACAC	GTGTGCTGTATGTTTcCTGTGAACCCAAAAGG
D921N	GACATAAATTATCACaATGCATTCCCTTGA	TCAAGGAATGCATtGTGATAATTTATGTC
D925N	CACGATGCATTCCTTaATCCATTACTGAG	CTCAGTAATGGATtAAGGAATGCATCGTG
DD921-925NN	CACaATGCATTCCTTaATCCATTACTGAG	CTCAGTAATGGATtAAGGAATGCATtGTG
Rat snake TRPA1	Sense primer (5'→3')	Antisense primer (5'→3')
Q895E	CTTCTTGGTTCACAGgAAACATATGGCACTCC	GGAGTGCCATATGTTTcCTGTGAACCAAGAAG
E919Q	CCGTcAGGCTTTCCTTGAACCAATG	AAGGAAAGCCTgACGGTAGTTGTTATCTCC
E923Q	TTCCTTcAACCAATGCTCGCTGATAAACTC	CATTGGTTgAAGGAAAGCCTCACGGTAG
EE919-923QQ	CCGTcAGGCTTTCCTTcAACCAATG	CATTGGTTgAAGGAAAGCCTgACGGTAG

Figure 1

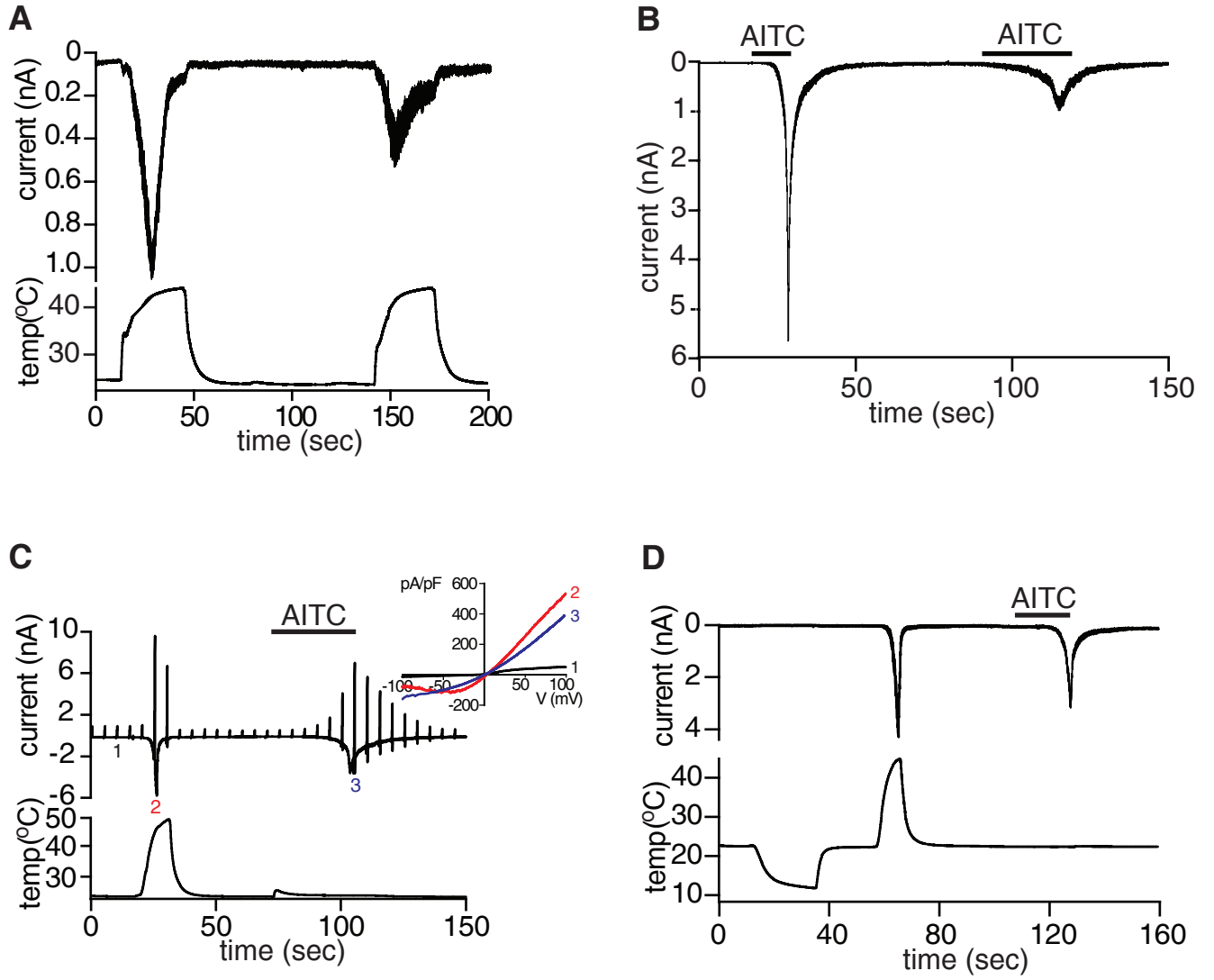


Figure 2

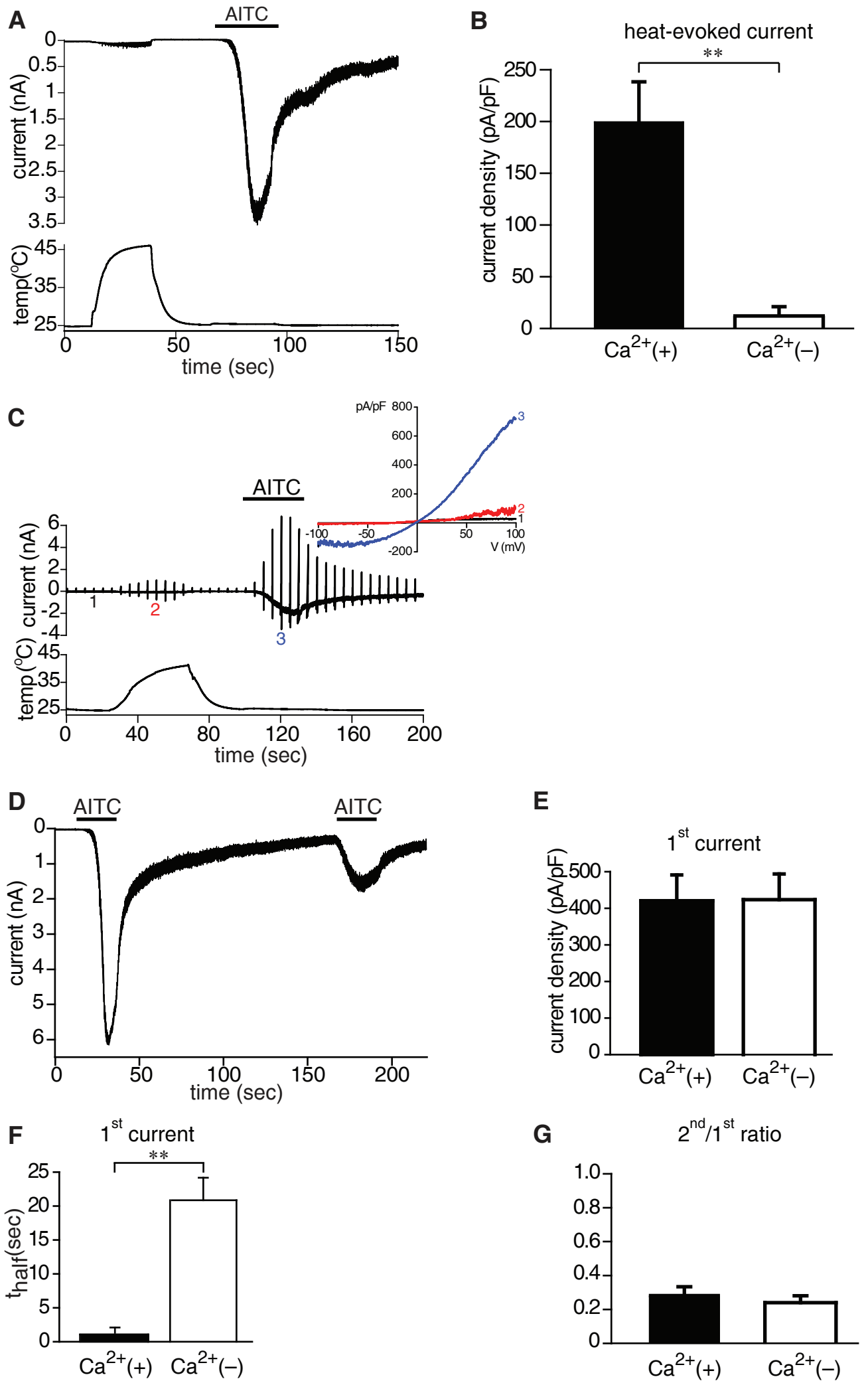


Figure 3

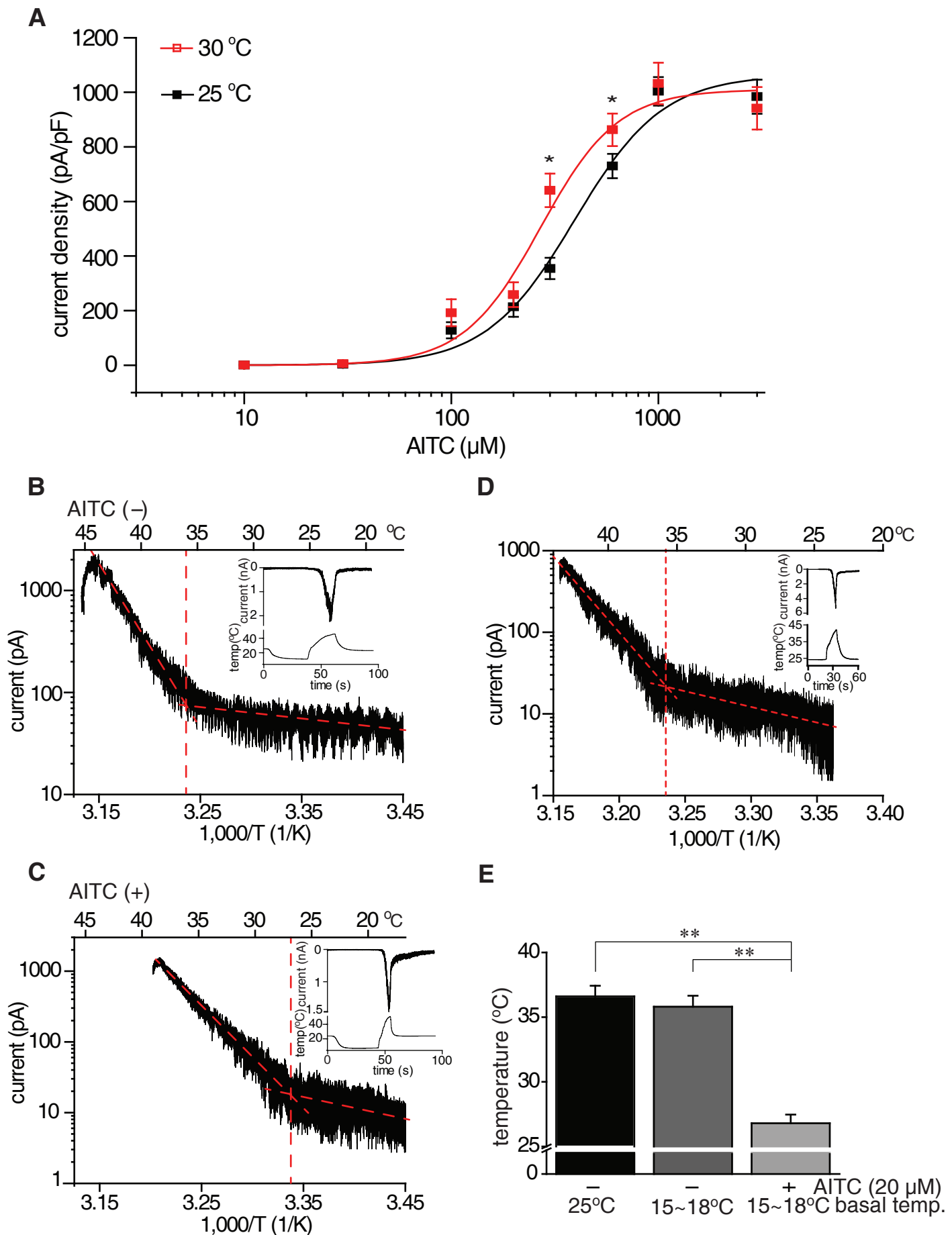


Figure 4

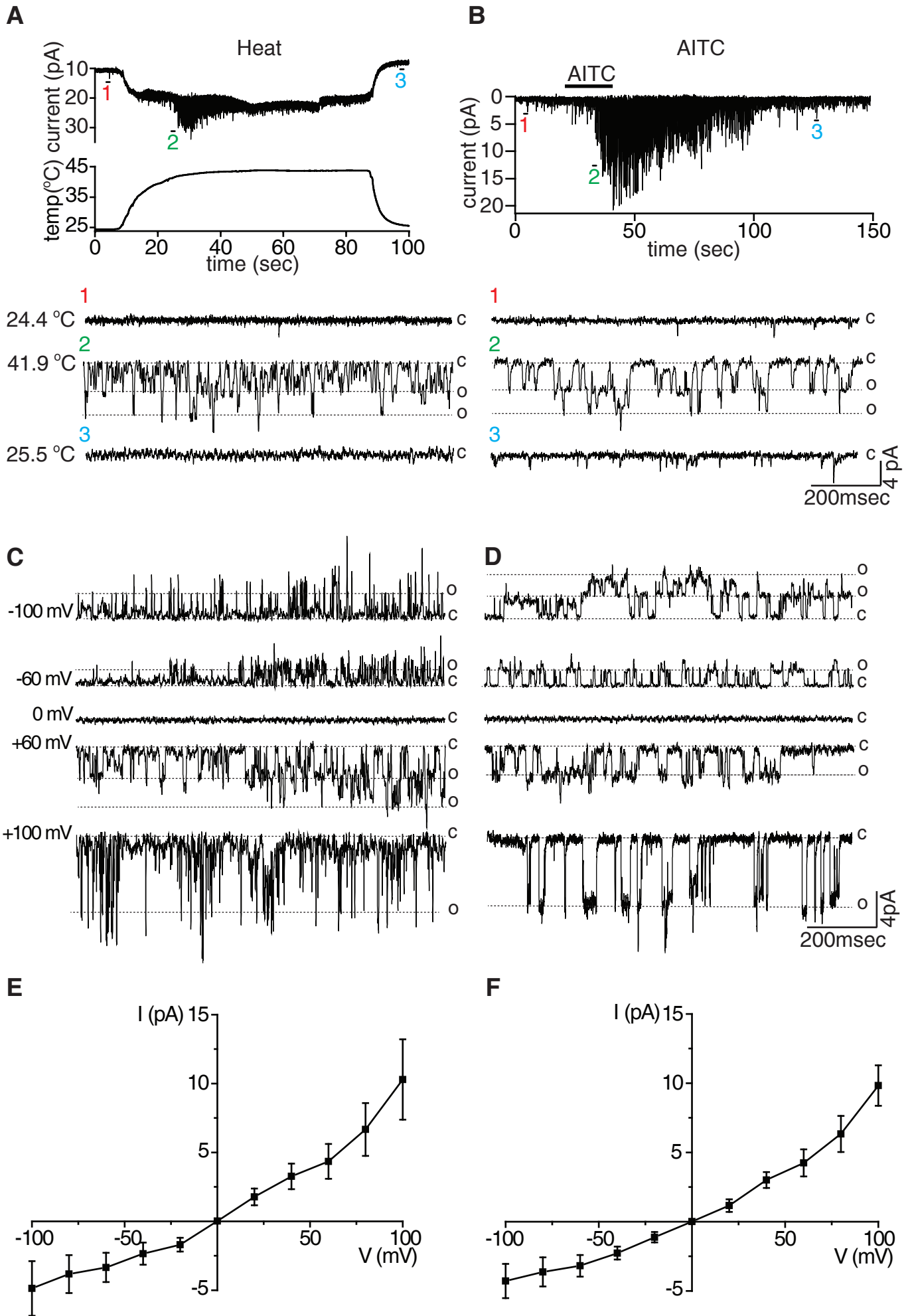


Figure 5

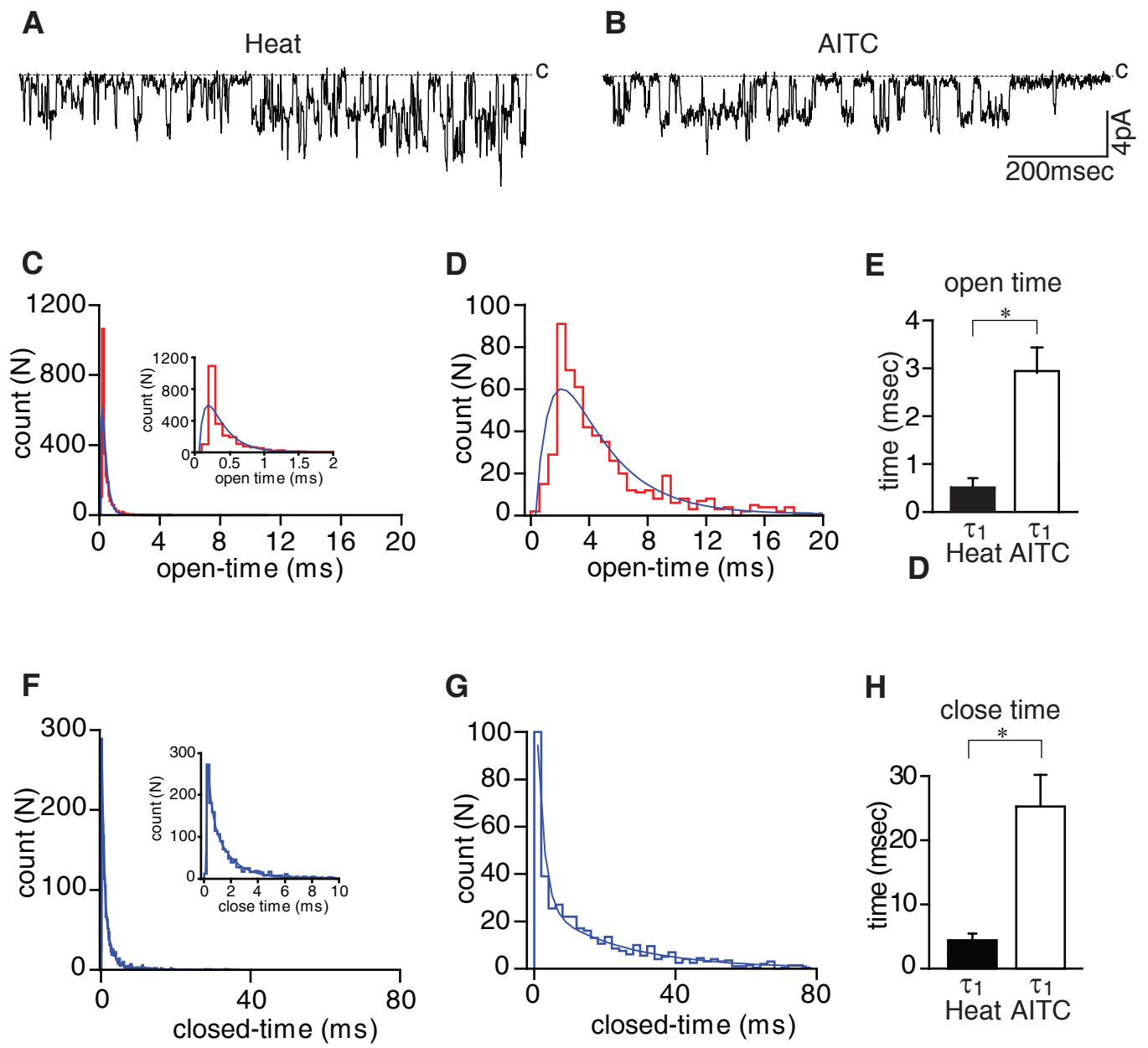


Figure 6

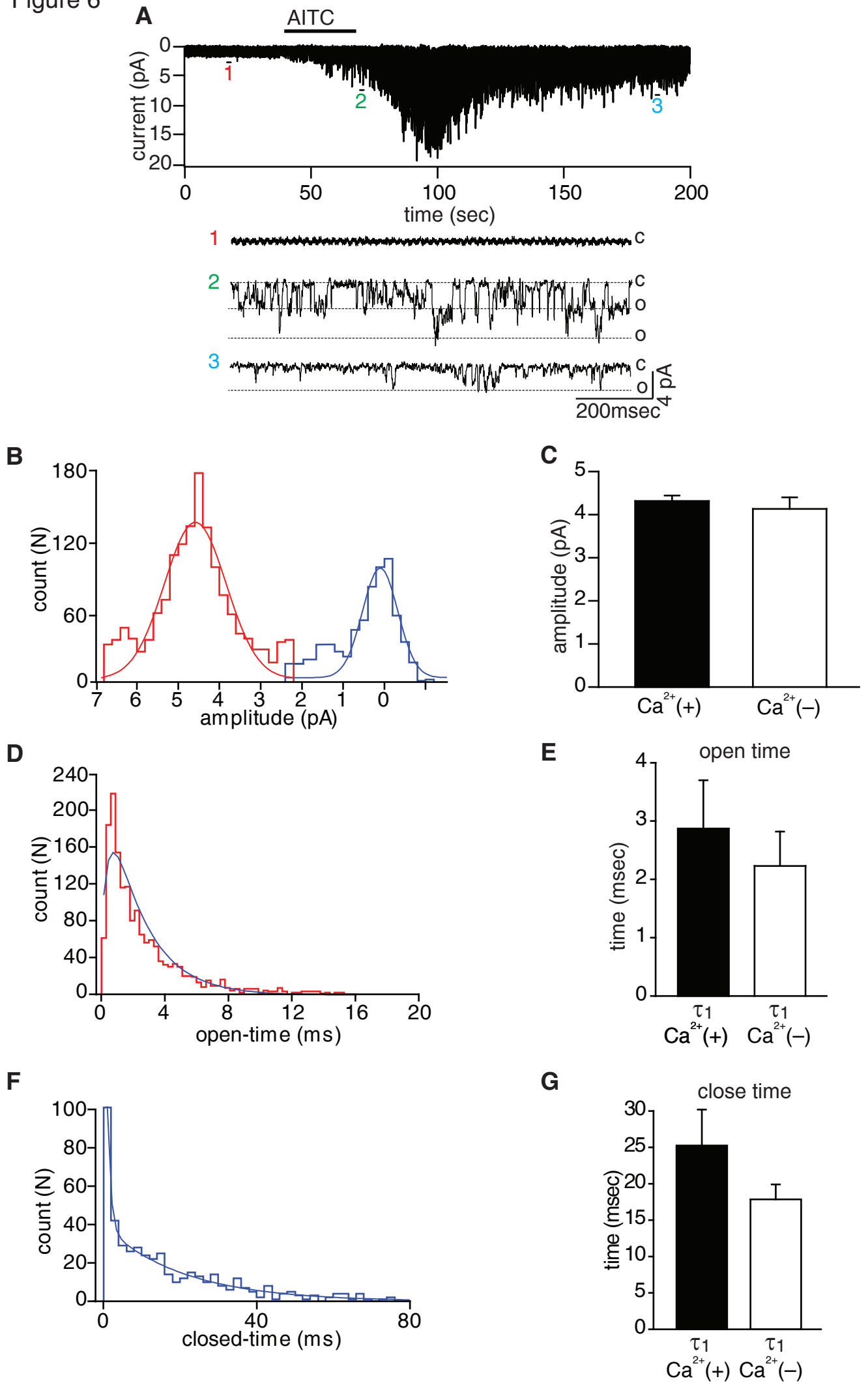


Figure 7

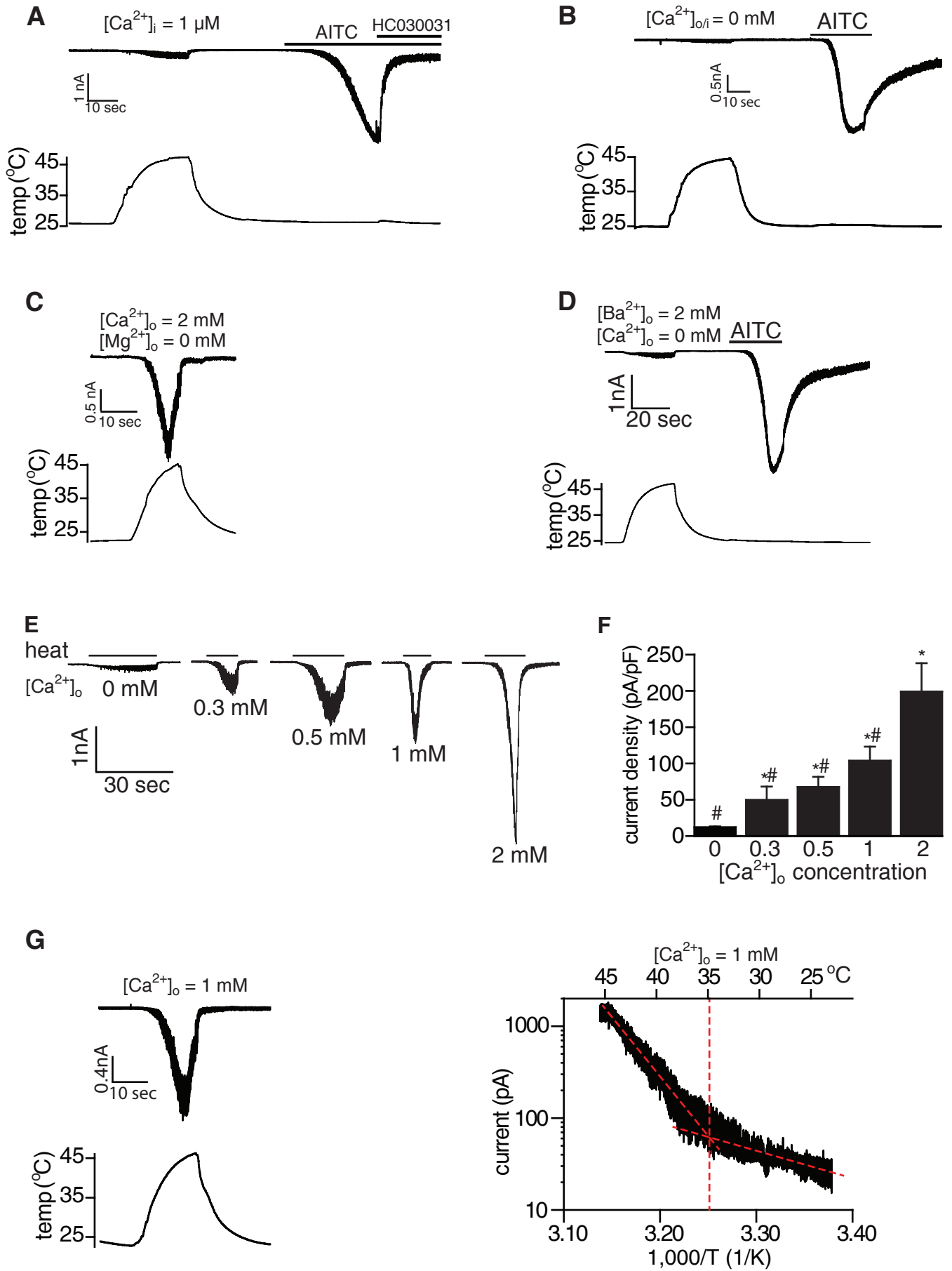


Figure 7 (continued)

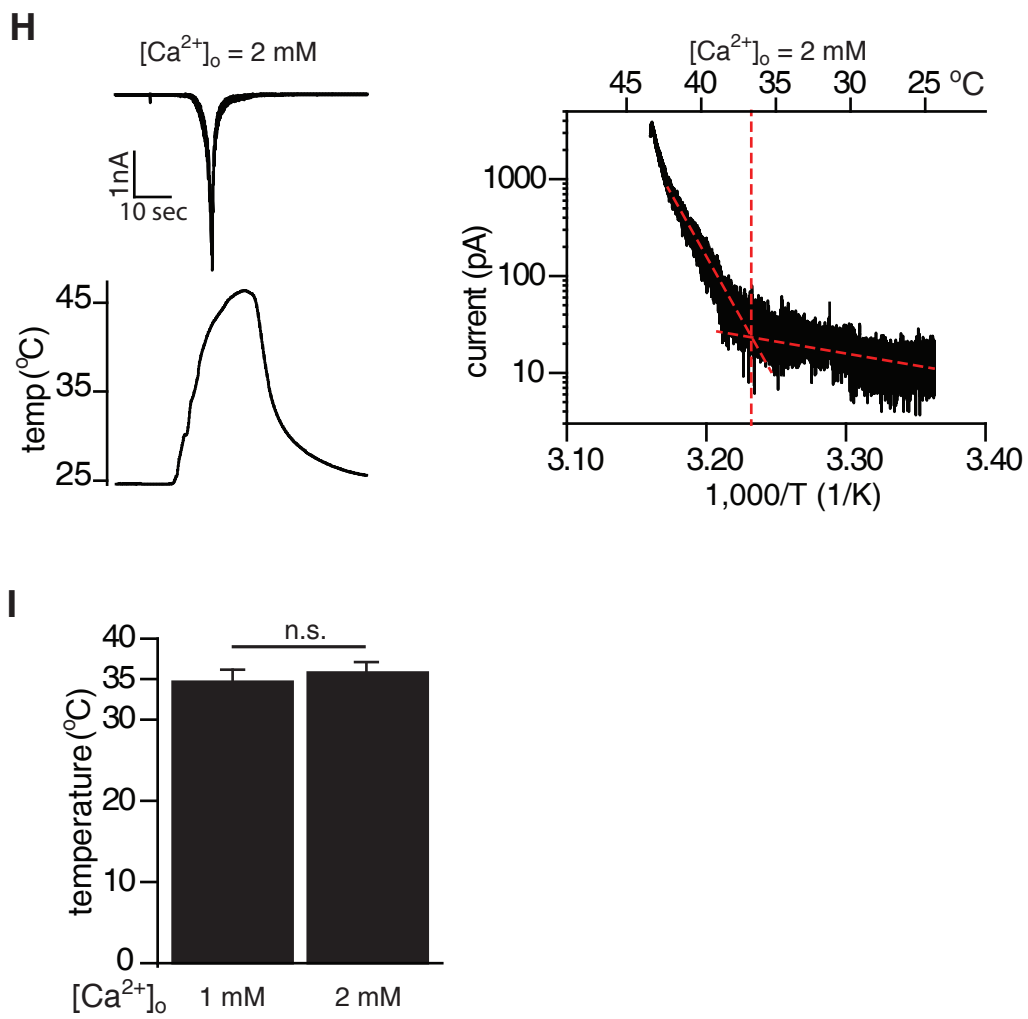
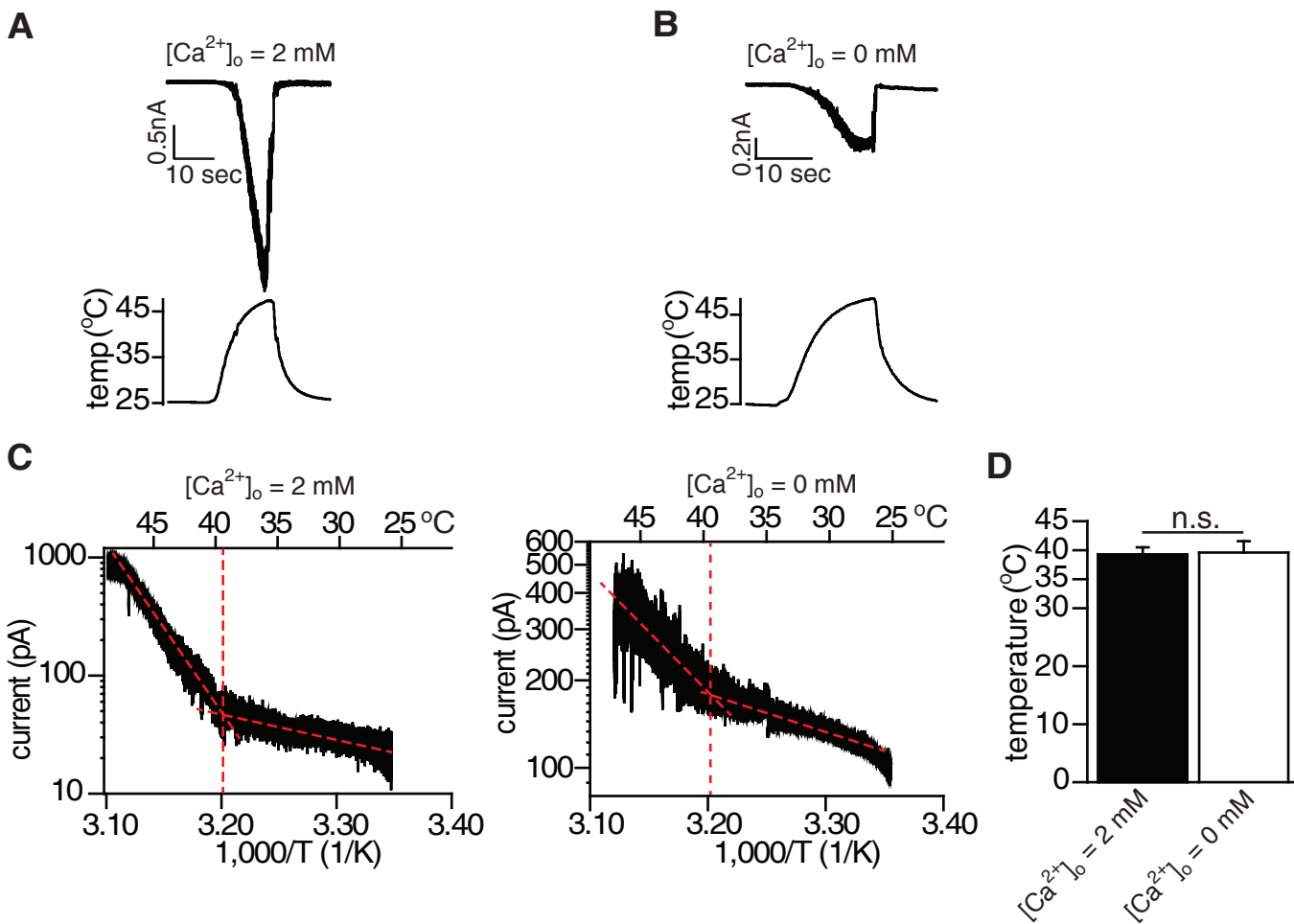


Figure 8

chTRPA1



rsTRPA1

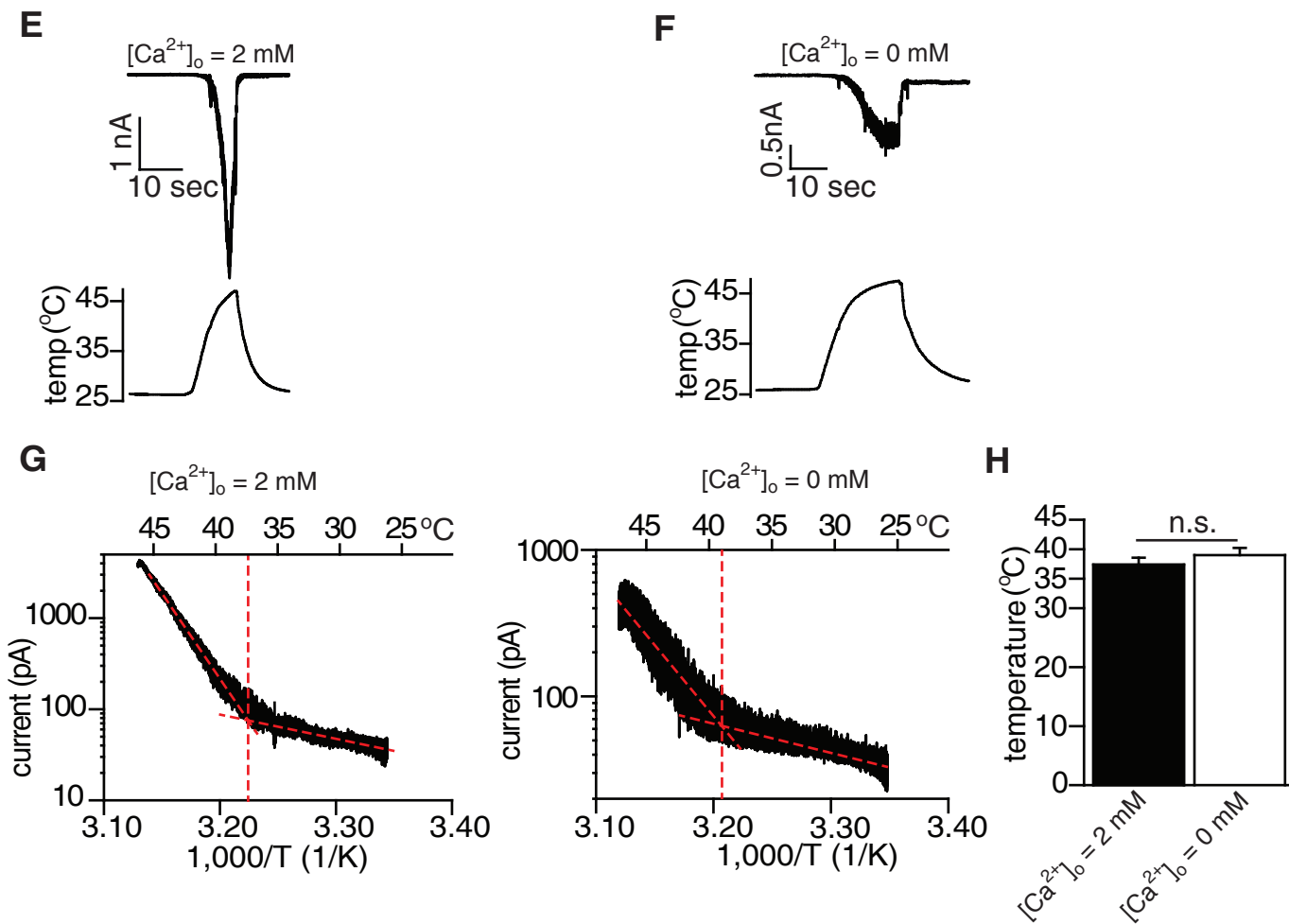


Figure 9

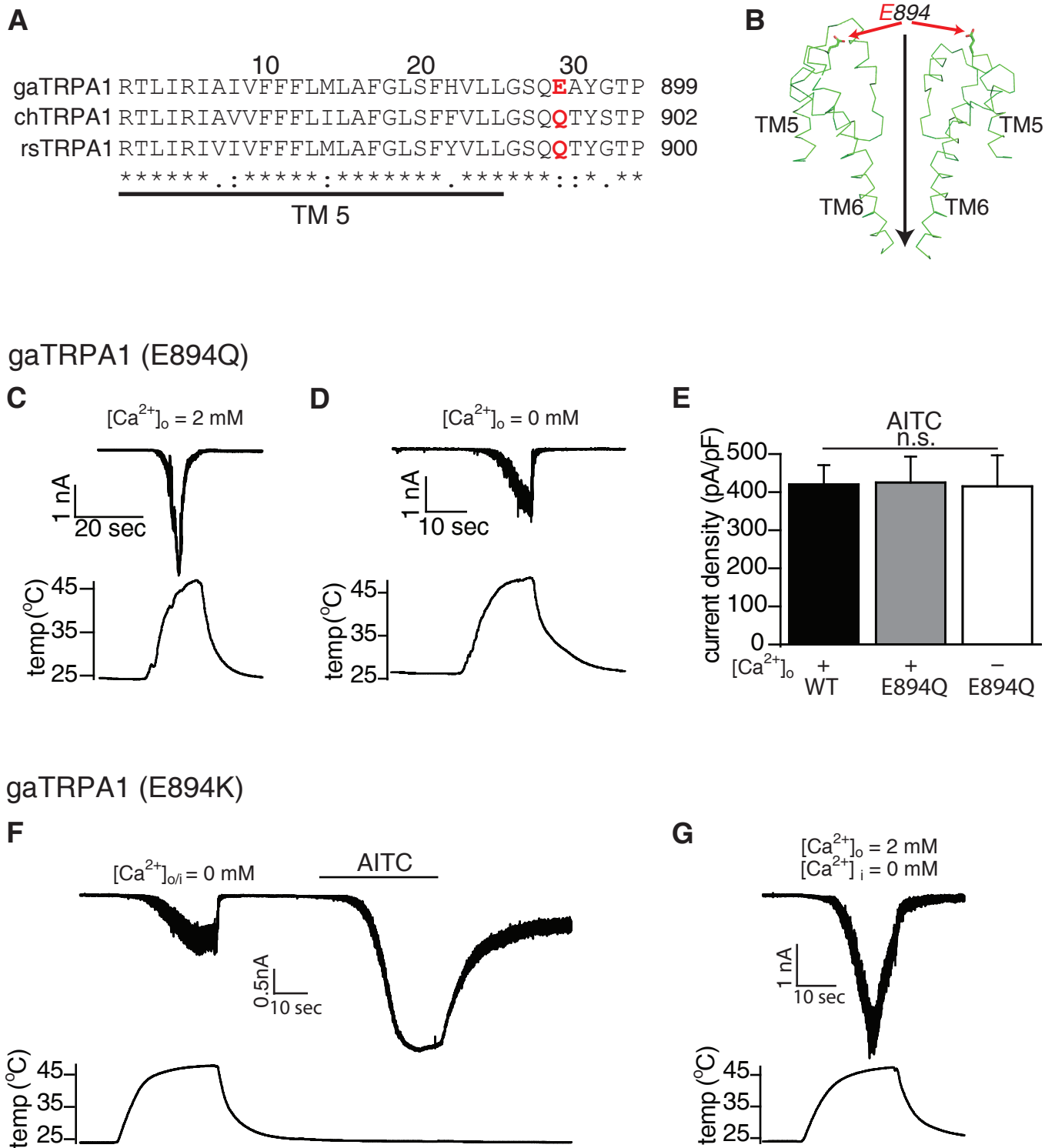
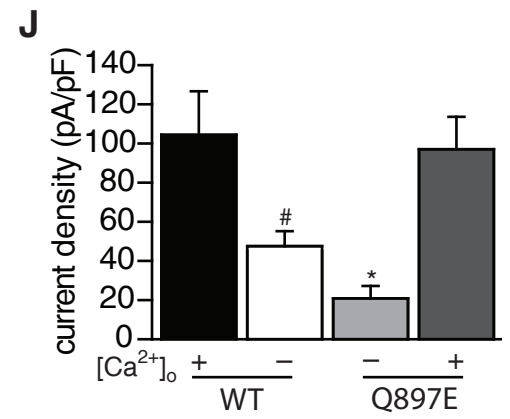
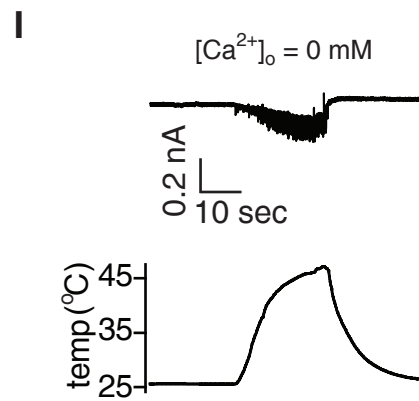
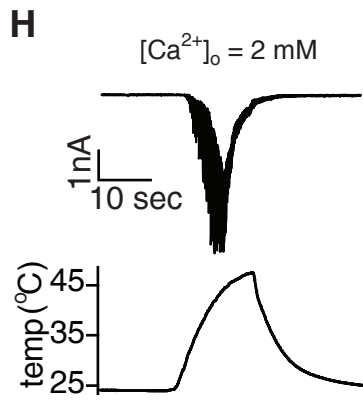


Figure 9 (continued)

chTRPA1 (Q897E)



rsTRPA1 (Q895E)

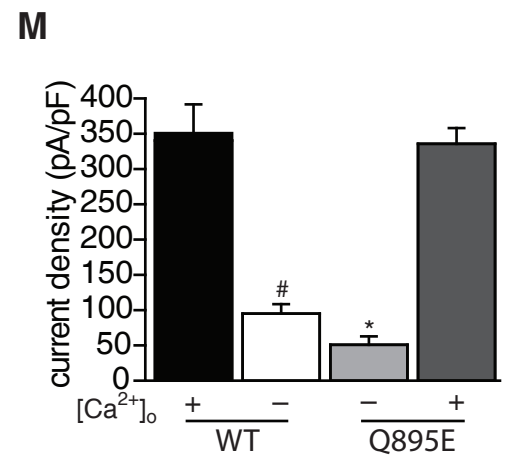
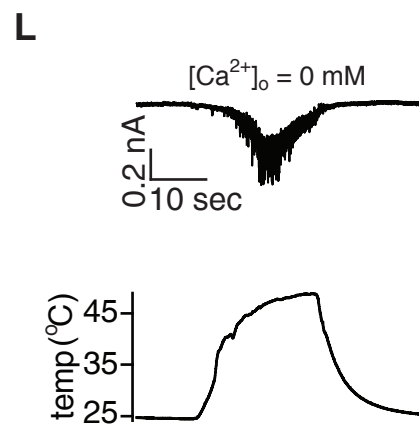
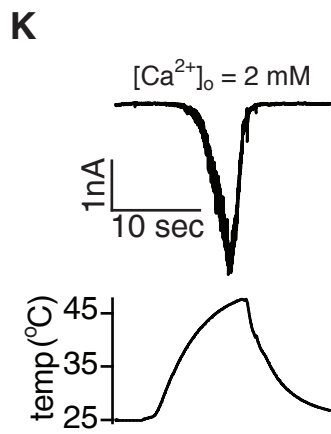
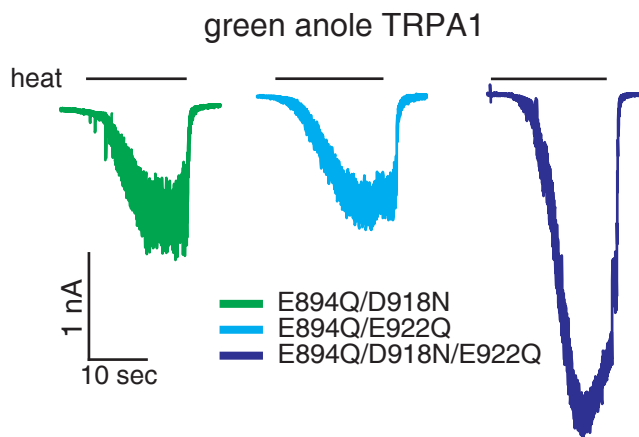


Figure 10

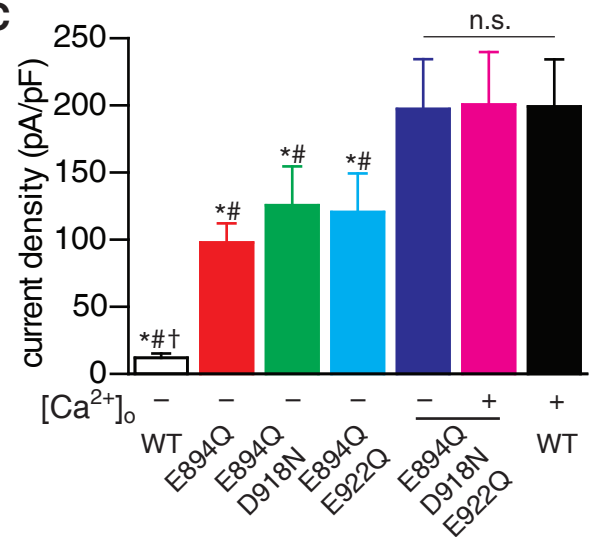
A

	TM 5	Pore helix 1	Pore helix 2	TM 6	
gaTRPA1	SFHVLLGSQ	E AYGTPYLSVMQTFAMMLGDINYH	D AF L E PMLTNKLPYPLLSYIIL		939
chTRPA1	SFFVLLGSQQ	TYSTPLLSVMKTFAMMLGDINYH	D AF L D PLLSSELPYPFLSYTVL		942
rsTRPA1	SFYVLLGSQQ	TYGTPYLSVMQTFSMIGDNNYR	E AF L E PMLADKLPFPFLSFIIIL		940
	** .*****:	: : .** *****:***:***:***	** : :***:***:***:***	** : :***:***:***:***:***:***:***:***	: *

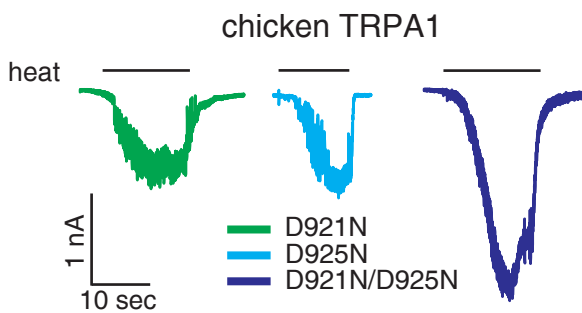
B



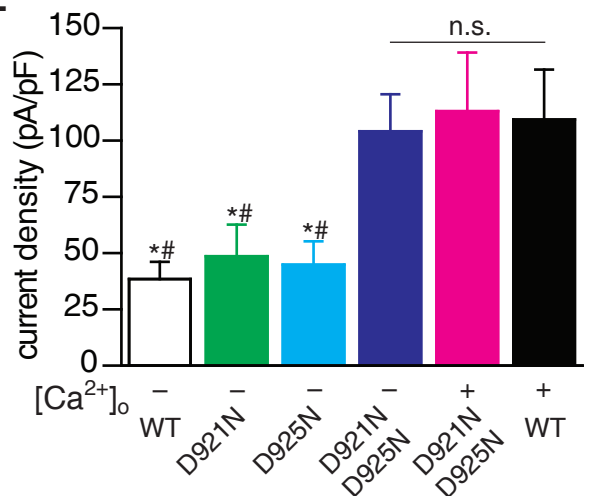
C



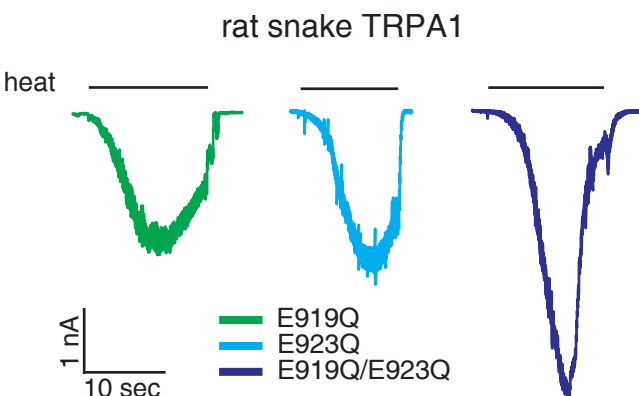
D



E



F



G

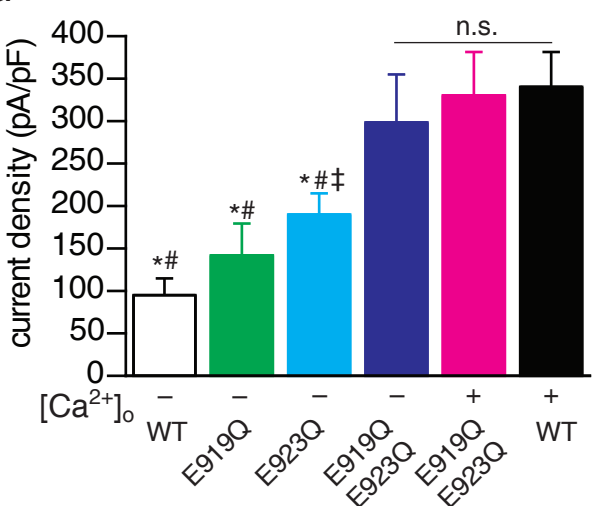
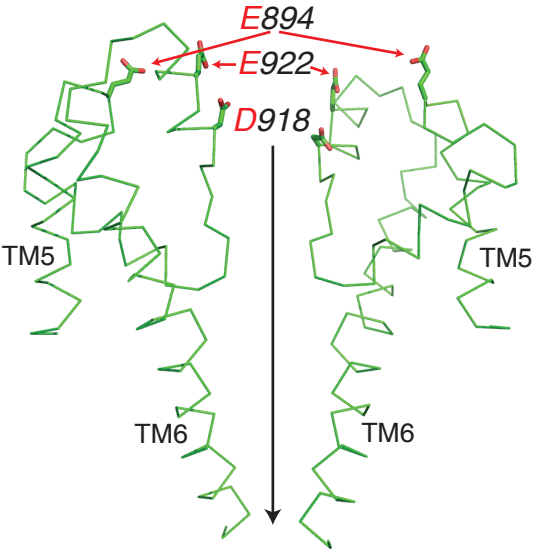


Figure 11



Acknowledgements

Foremost, I would like to express my sincere gratitude to my advisor Professor Makoto Tominaga for his continuous support and help during my PhD study and research, as well as for his patience and tremendous knowledge. Professor Tominaga's guidance and motivation helped me both in my research and my life in Japan. I am thankful to God that I did my PhD study and research under Professor Tominaga's guidance. I also thank Assistant Professor Dr. Kunitoshi Uchida, Assistant Professor Dr. Shigeru Saito, and Dr. Yiming Zhou for their insightful comments and guidance for my experiments, as well as Lab Technician Claire T. Saito for her teaching and help with molecular biology techniques.

Second, I thank Professor Sabirov R.Z. and Dr. Petr Merzlyak for their encouragement and kind support during my PhD study and life in Japan.

My sincere thanks also go to my former and current laboratory members for their discussions, help, and support, and for the all fun we had in the last five years.

Last, I would like to thank my family; my parents who supported me spiritually throughout my PhD study, and my brother and sisters for their patience and kindness.